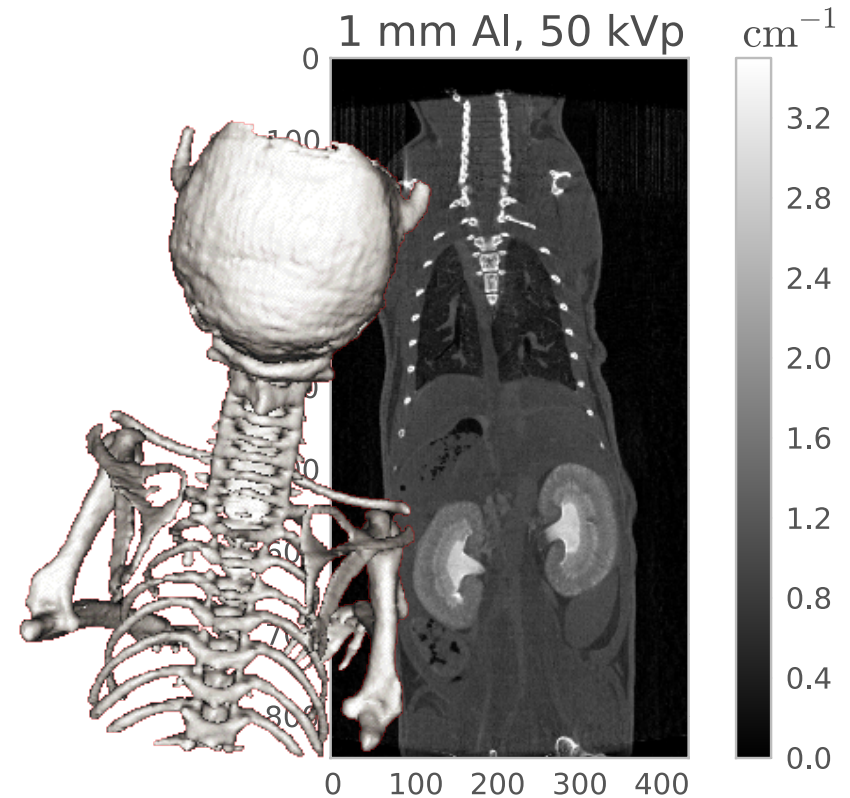
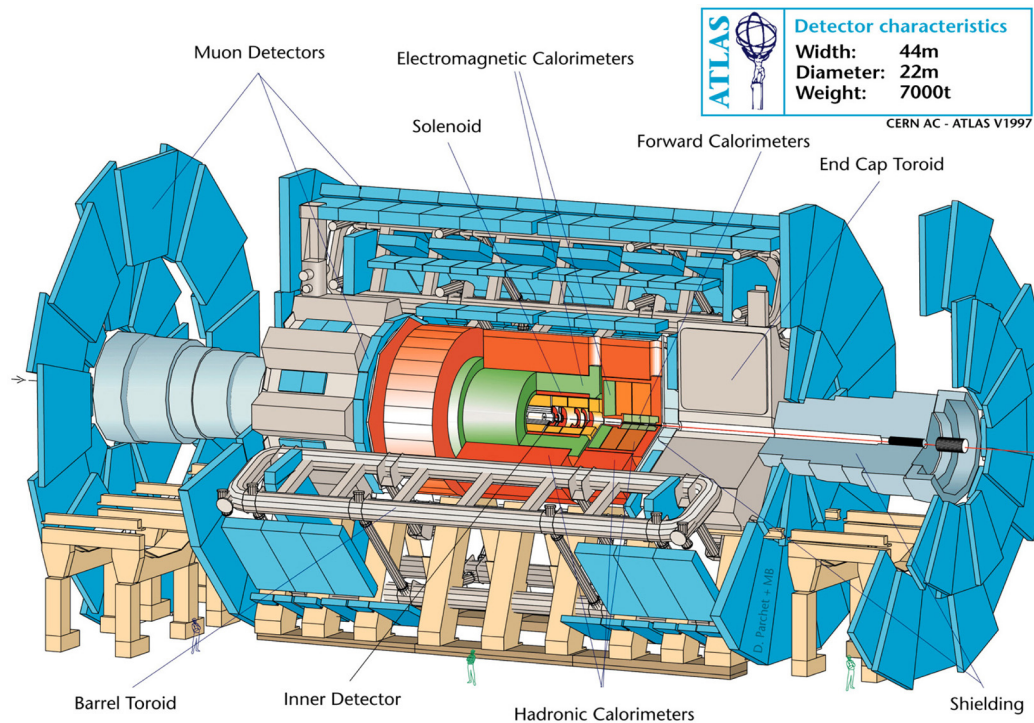




Detectors for X-ray imaging

Pr Christian MOREL, PhD



Discovery of X-rays (1895)



Wilhelm Roentgen (1845-1923)
Nobel Prize in Physics (1901)



22 Dec 1895 – published in the
New York Times on 16 Jan 1896

Development of radiology (roentgenology)



Hôpital Tenon (Paris, 1897)
Antoine Béclère (1858–1939)



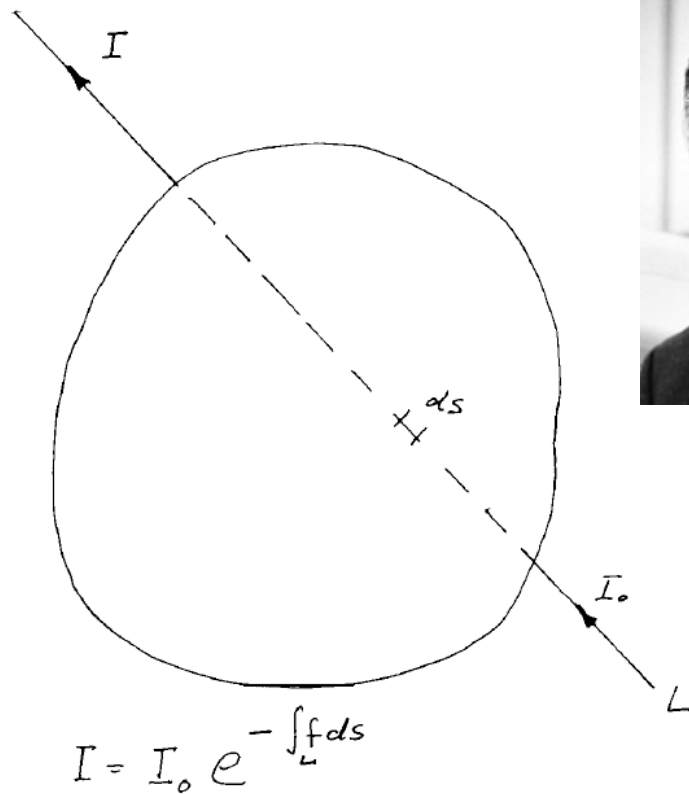
Radiological Renault «Petite Curie» (1916)
Marie Curie (1867-1934)



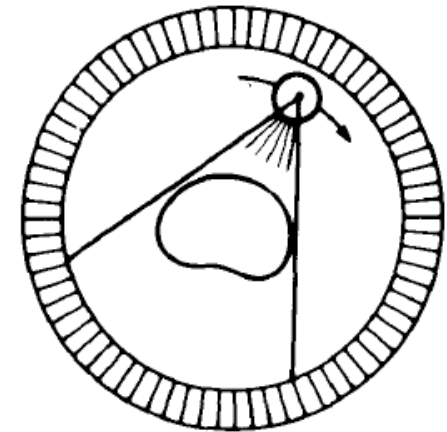
Development of Computerized Tomography (CT)

Rediscovery of the Radon solution for reconstruction from projections (Cape Town, 1963)
Allan McLoed Cormack (1924-1998)

Development of the first CT scanner at EMI (London, 1972)
Sir Godfrey Newbold Hounsfield (1919-2004)



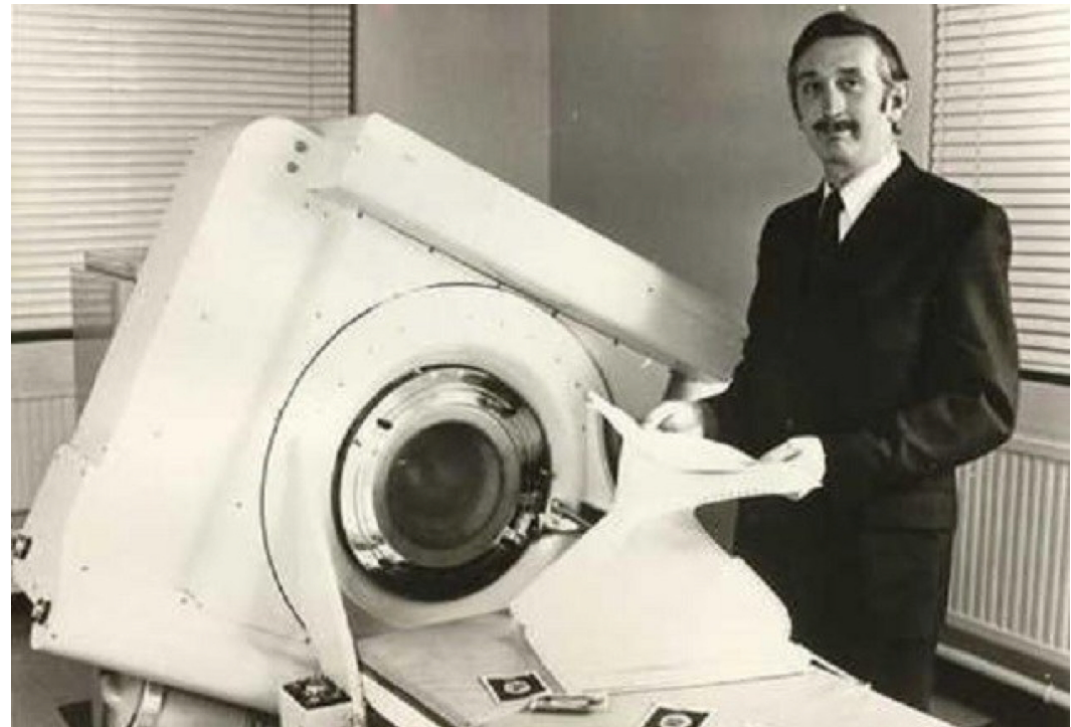
300 detectors
Scan time 2 - 4 seconds



700 stationary detectors
Scan time 2 - 4 seconds

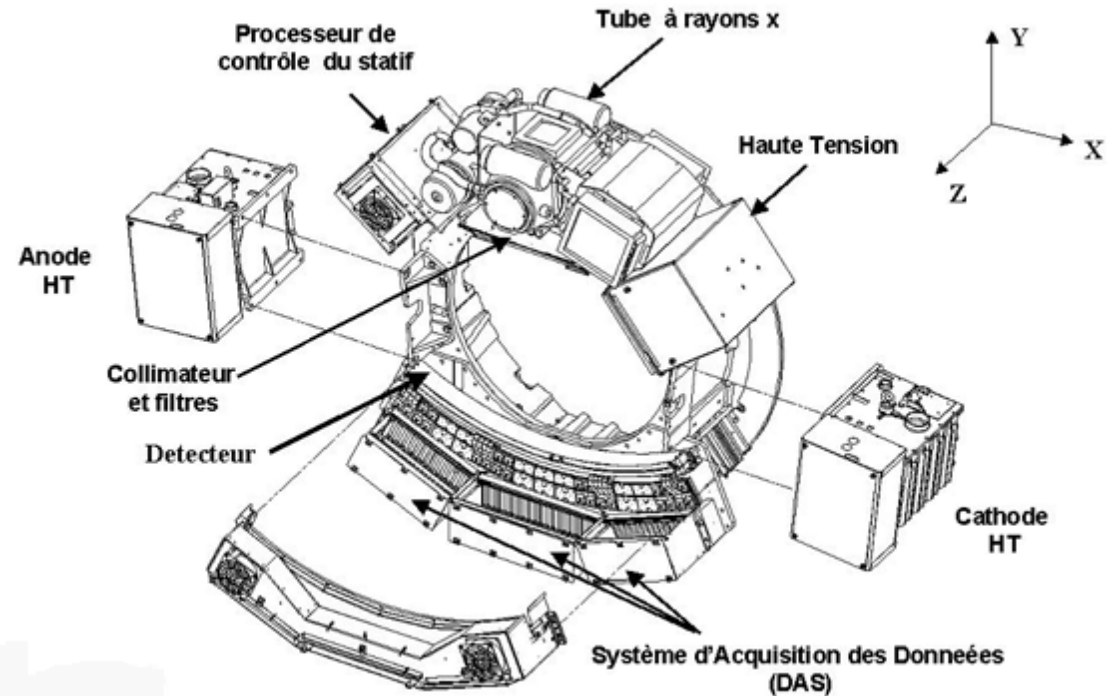
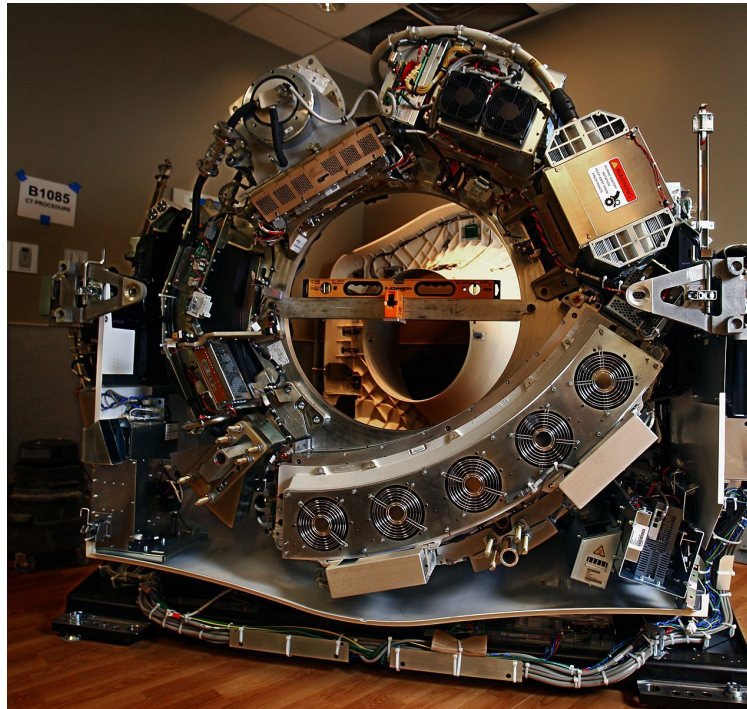
Nobel Prize in Medicine (1979)

Computerized Tomography (CT)



G. Hounsfield, J. Ambrose
(Atkinson Morley Hospital, London, 1/10/1971)

X-ray CT scanner



<i>Diagnostic procedure</i>	<i>Typical effective dose (mSv)</i>	<i>Equiv. no. of CXR</i>	<i>Approx. equiv. period of background radiation</i>
CXR	0.02	1	3 days
CT head	2.0	100	10 months
CT chest	8	400	3.6 years
CT abdomen/pelvis	10	500	4.5 years

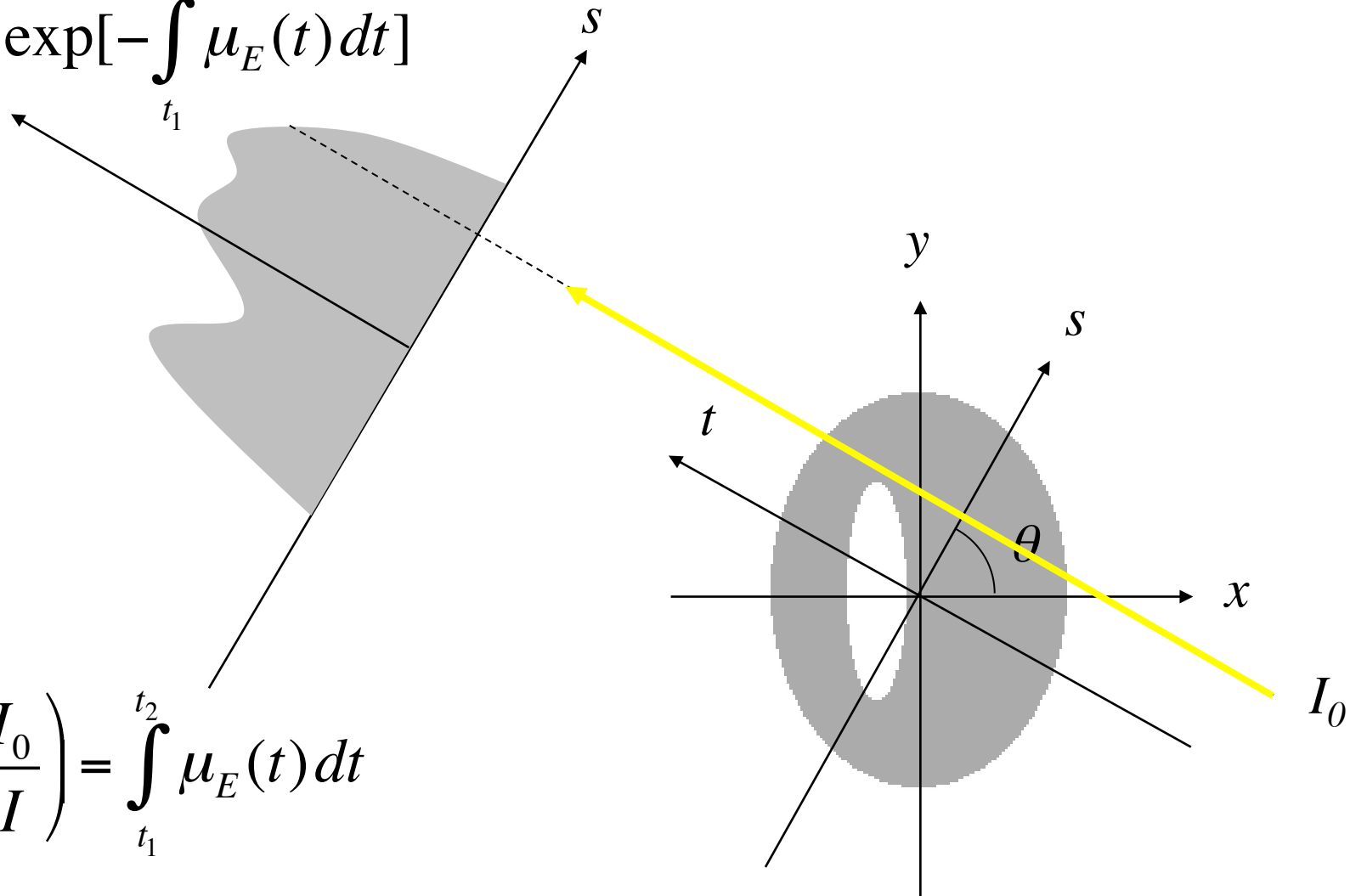
UK average background radiation = 2.2 mSv per year; regional averages range from 1.5 to 7.5 mSv per year.

Transmission tomography

Monochromatic case

$$I = I_0 \exp\left[-\int_{t_1}^{t_2} \mu_E(t) dt\right]$$

$$\ln\left(\frac{I_0}{I}\right) = \int_{t_1}^{t_2} \mu_E(t) dt$$



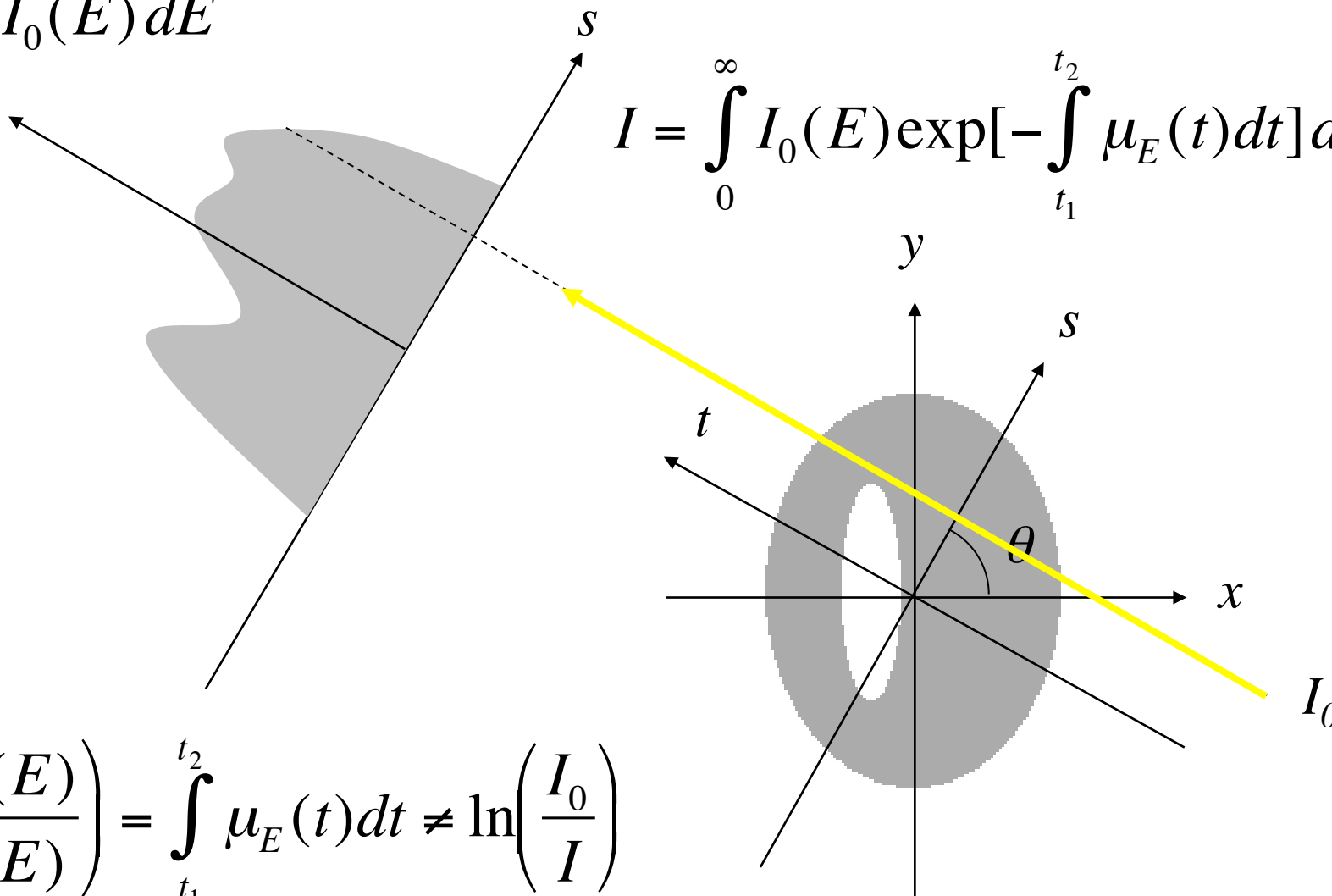
Transmission tomography

Polychromatic case

$$I_0 = \int_0^{\infty} I_0(E) dE$$

$$I = \int_0^{\infty} I_0(E) \exp\left[-\int_{t_1}^{t_2} \mu_E(t) dt\right] dE$$

$$\ln\left(\frac{I_0(E)}{I(E)}\right) = \int_{t_1}^{t_2} \mu_E(t) dt \neq \ln\left(\frac{I_0}{I}\right)$$

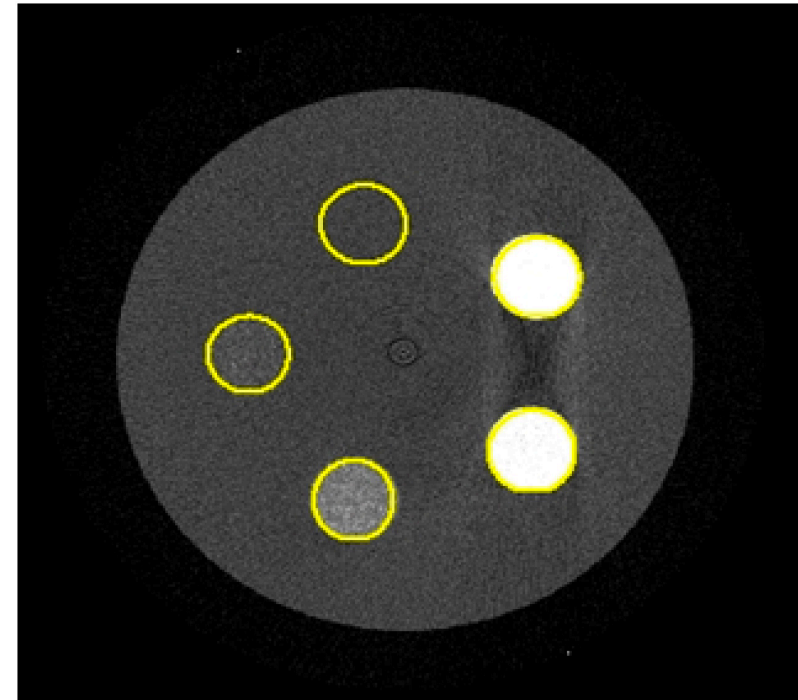
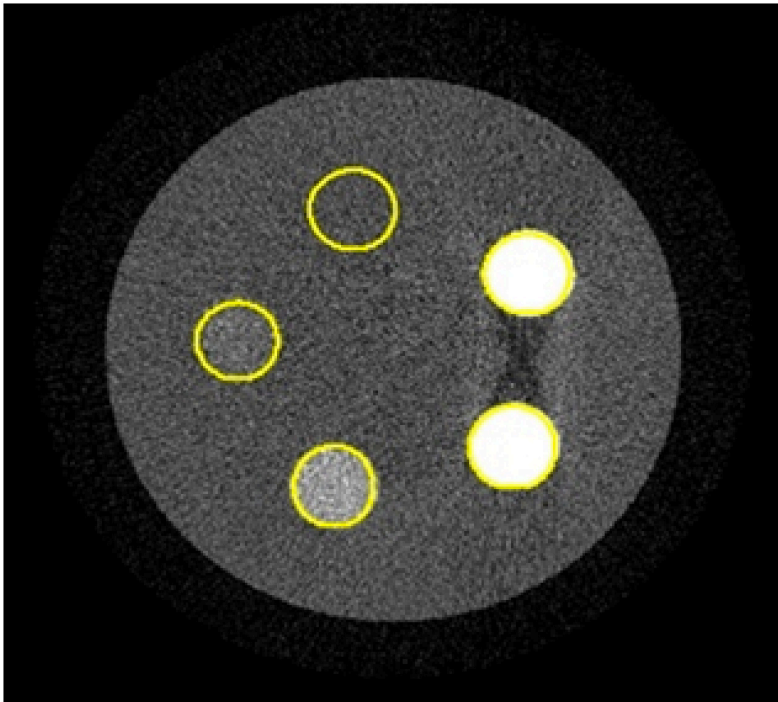


Transmission tomography

$$I_0 = \int_0^{\infty} I_0(E) dE$$

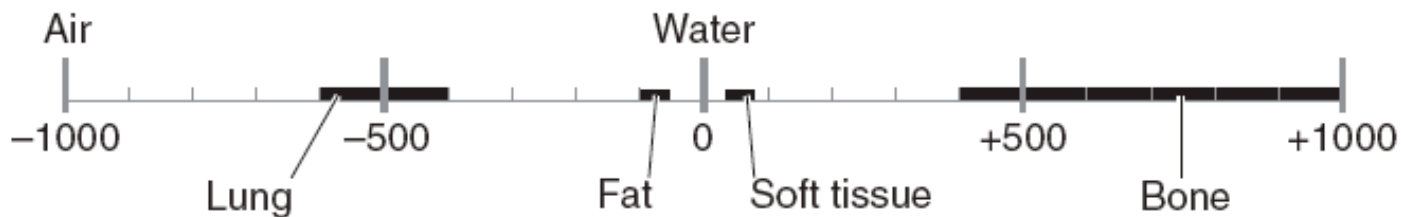
Polychromatic case -> beam hardening

$$I = \int_0^{\infty} I_0(E) \exp\left[-\int_{t_1}^{t_2} \mu_E(t) dt\right] dE$$

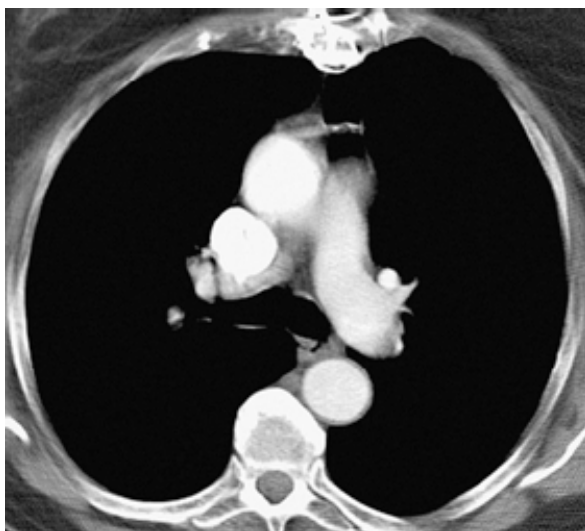


$$\ln\left(\frac{I_0(E)}{I(E)}\right) = \int_{t_1}^{t_2} \mu_E(t) dt \neq \ln\left(\frac{I_0}{I}\right)$$

Hounsfield Units (HU)



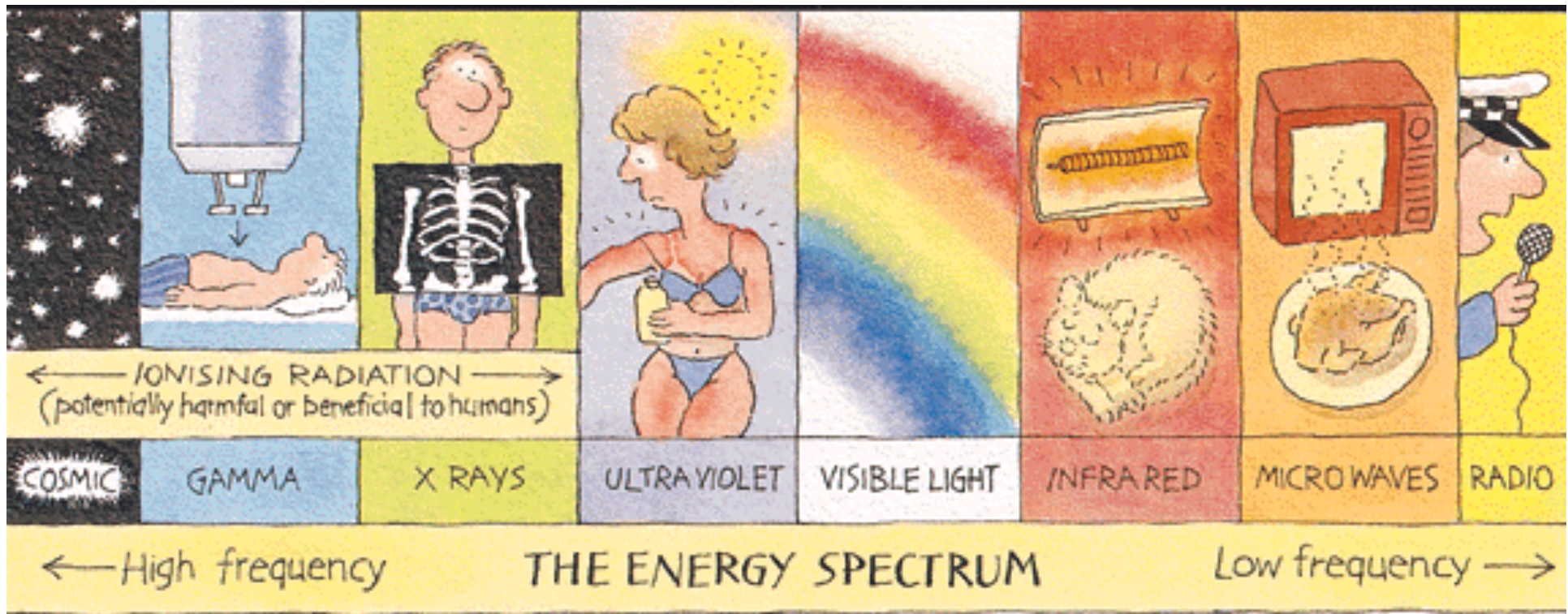
Bone	+400 → +1000
Soft tissue	+40 → +80
Water	0
Fat	-60 → -100
Lung	-400 → -600
Air	-1000



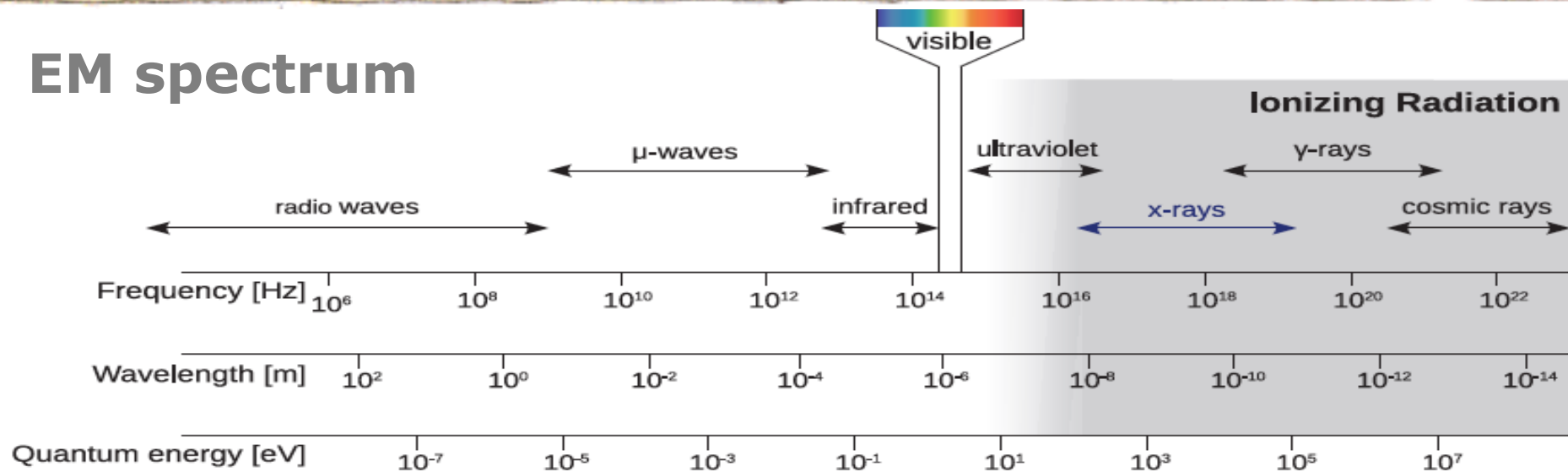
[40-390] HU



[-600-900] HU



EM spectrum



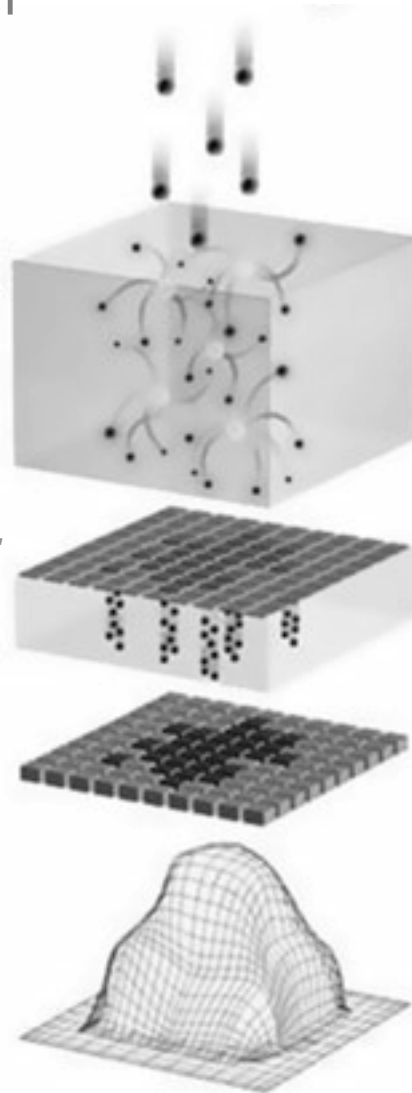
X-ray detection paradigm

Indirect detection

Scintillator or phosphor screen
Radiation converted to light

Photodetector (e.g. PMT, photodiode, CCD camera or CMOS pixel)
Light converted to electric signal

Image

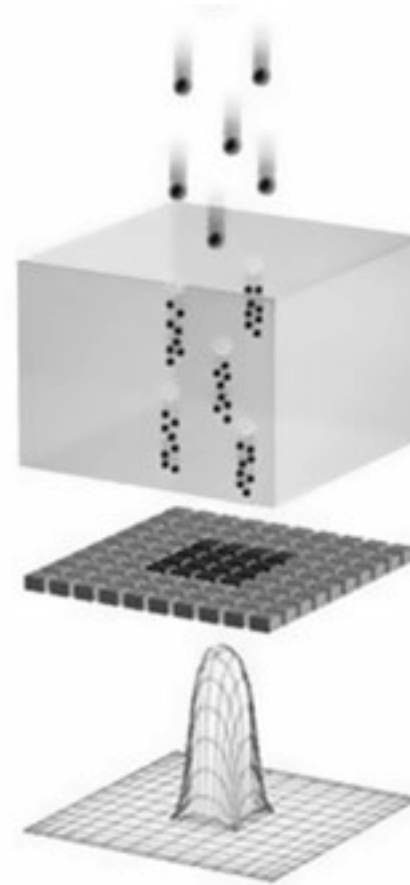


Direct detection

Gaz (e.g. Xe) or semiconductor (e.g. Si, CdTe, AsGa)

radiation converted to electric signal
Readout electronic circuit

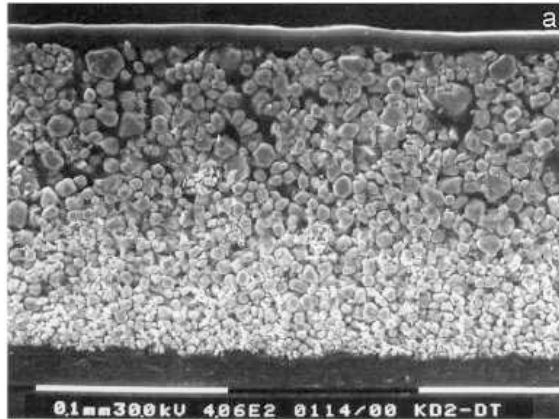
Image



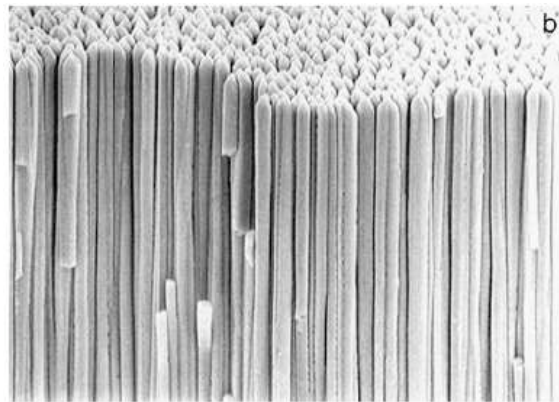
Courtesy: P. Russo and A. Del Guerra, INFN

Charge integration detectors

Converter



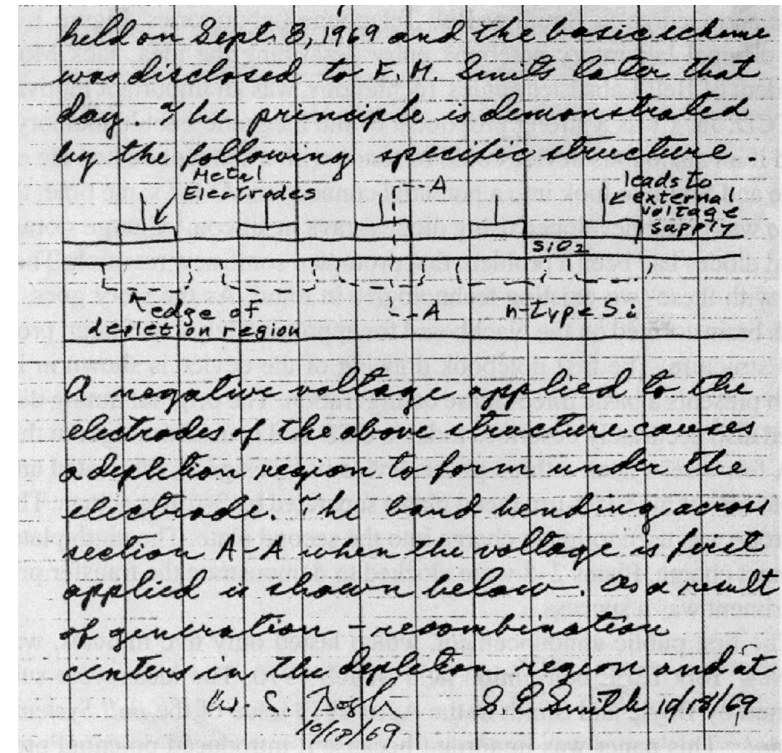
Gadolinium oxysulfide
(GOS or Gadox, Gd₂O₂S)



Cesium iodide (CsI)

Photodetector

Charged Couple Device (CCD) camera



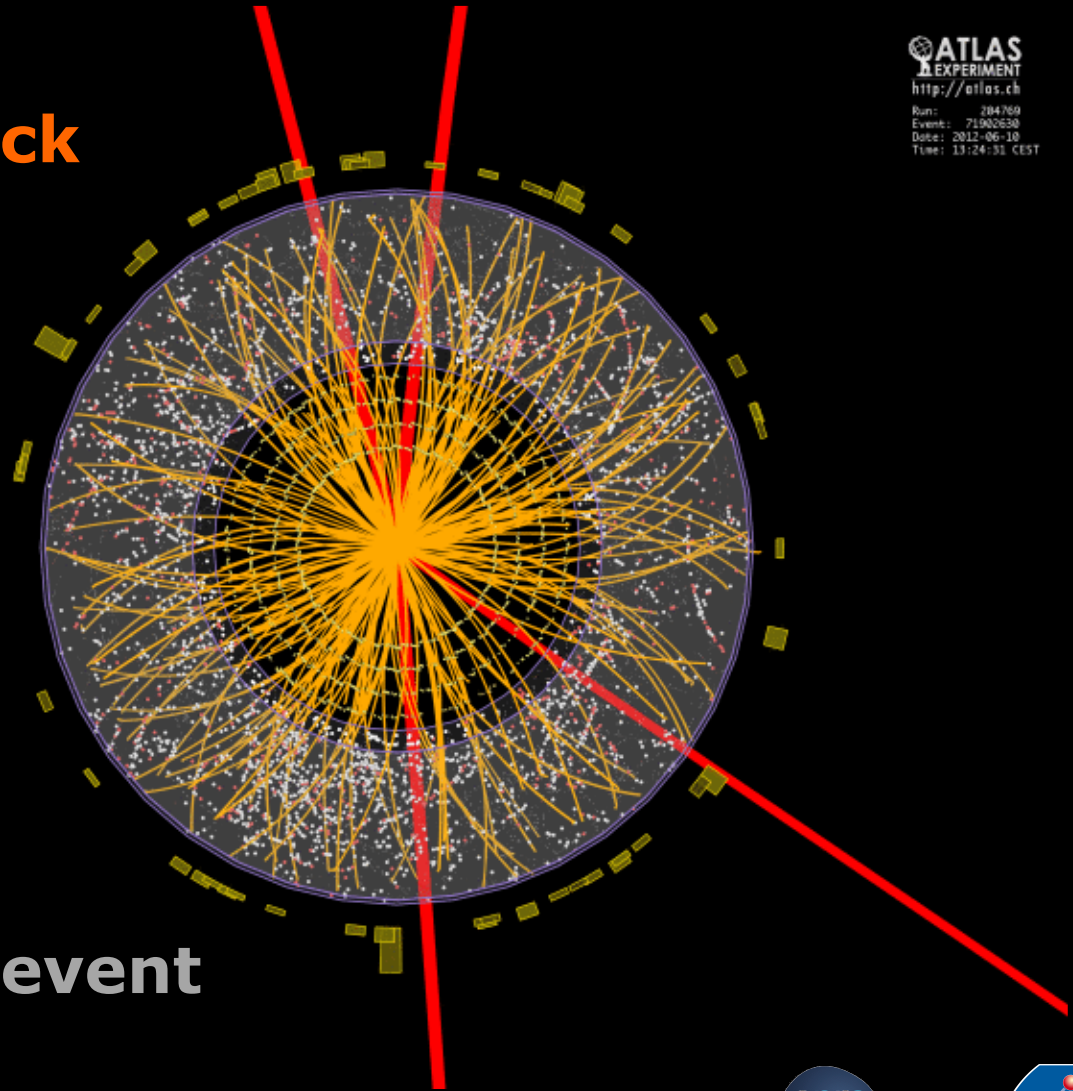
W.S. Boyle and G.E. Smith (Bell Labs, 1969)
Nobel Prize in Physics (2009)

Complementary Metal-Oxide Semiconductor
(CMOS) pixel

Trajectography at the LHC ATLAS experiment

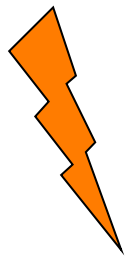
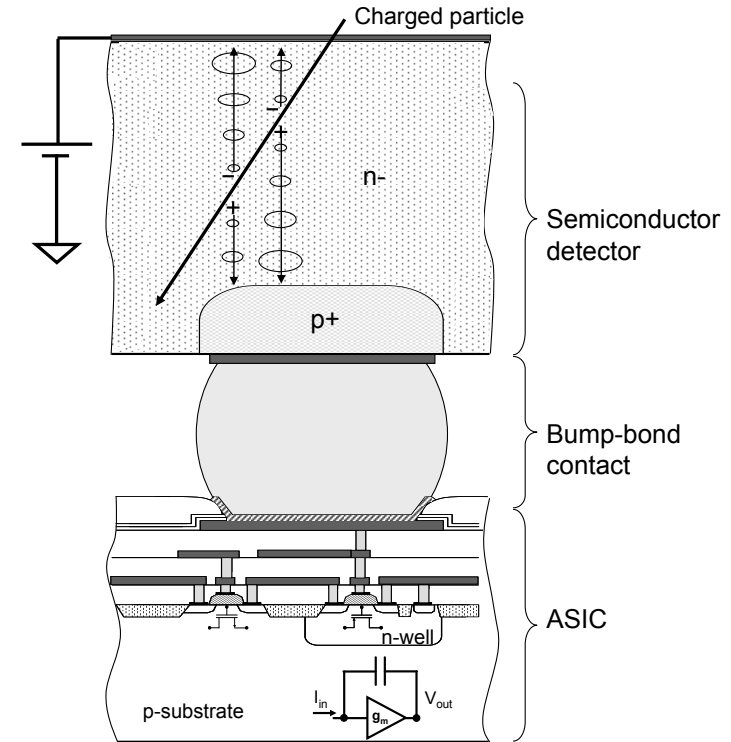
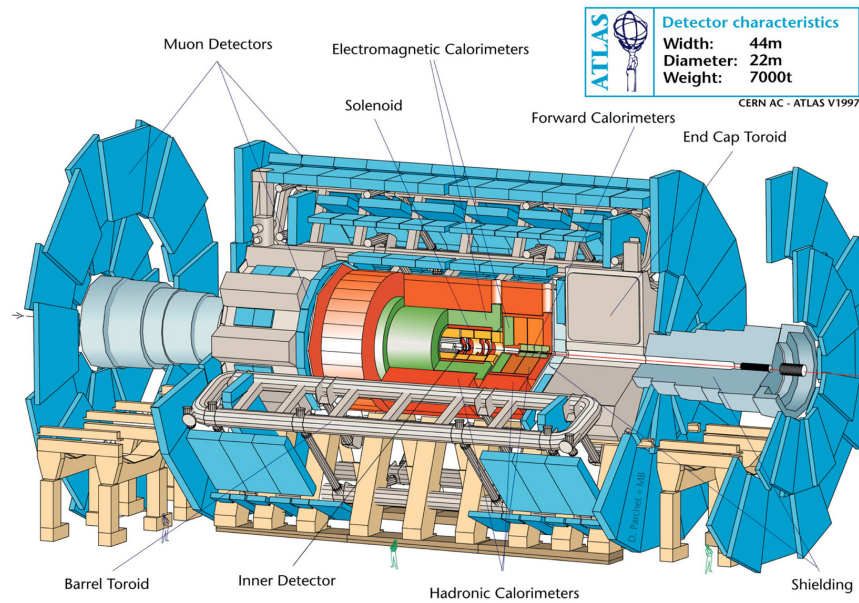
Thousands of particles
every 20 ns

Reconstruct every track
2D detectors



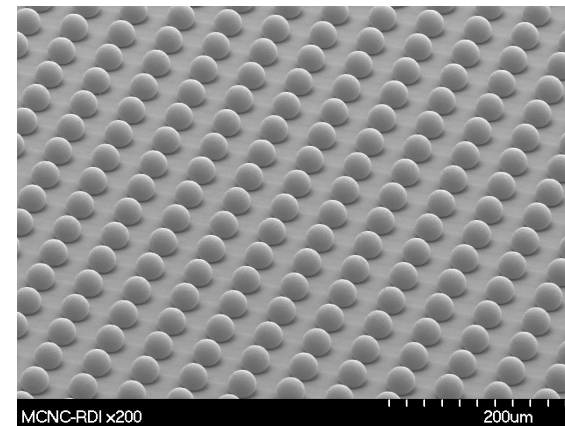
Higgs event

Hybrid Pixels: from LHC micro-vertex detectors to photon counting CT



- Noise suppression
- Energy selection
- Very high dynamics

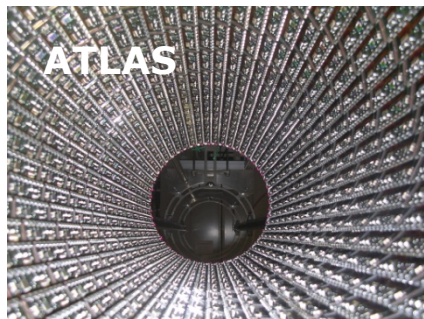
Reduce radiation dose
Improve contrast
Perform spectral analysis



Courtesy: M Campbell, Medipix Collaboration, CERN

XPAD: X-ray Pixel chip with Adaptable Dynamics

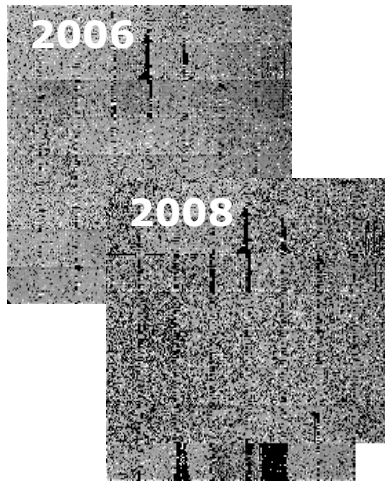
Start of the hybrid pixel project



ATLAS
50 x 400 μm^2 pixels



XPAD2.1 (2000)
XPAD2.2 (2002)
 ≈ 7 cm
330 x 330 μm^2 pixels



1991

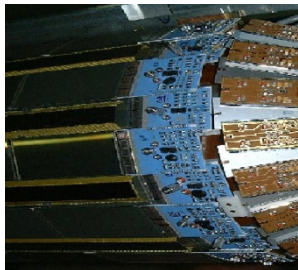
1998

2000

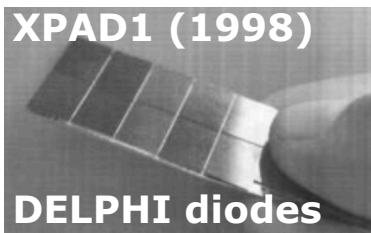


1996

DELPHI
World
première



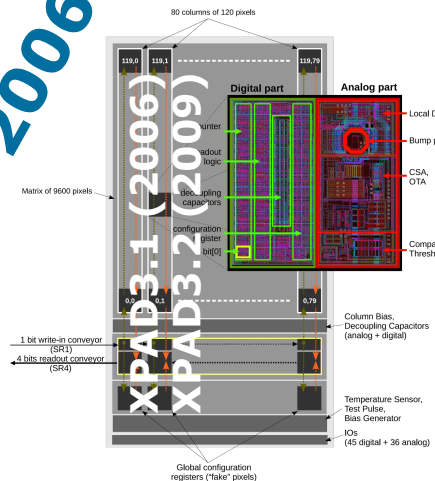
XPAD1: first hybrid pixel detector for X-ray detection



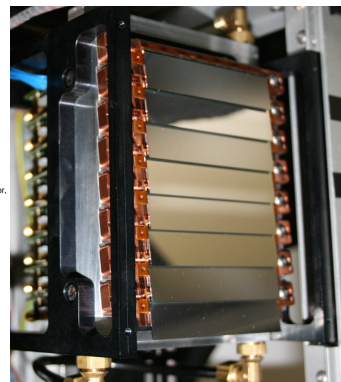
XPAD1 (1998)

DELPHI diodes

2006



130 x 130 μm^2 pixels

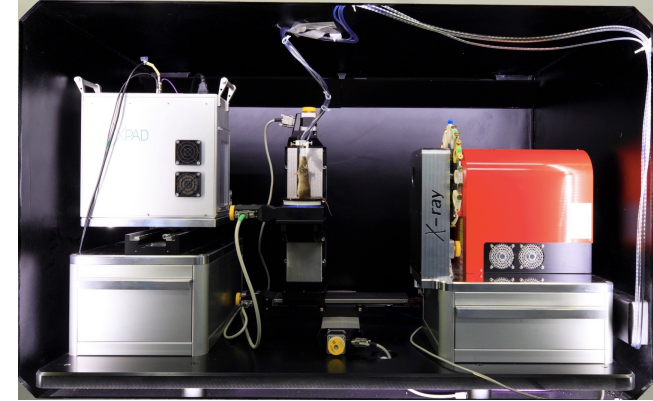
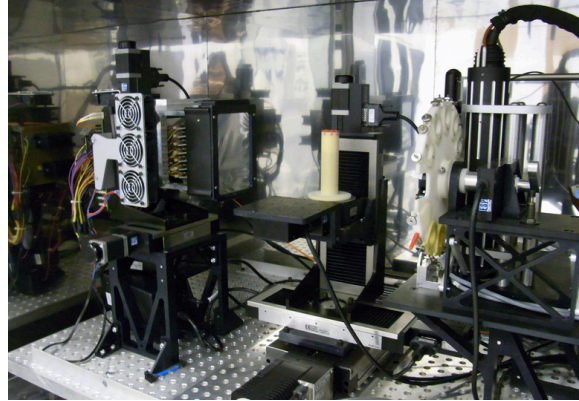
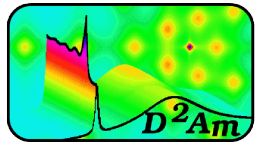


Delpierre, JINST 9 (2014) C05059

Ecole d'été Franco-Chinoise, Marseille, 2-10 Jul 2018



XPAD3 Si and CdTe hybrid pixels for X-ray detection



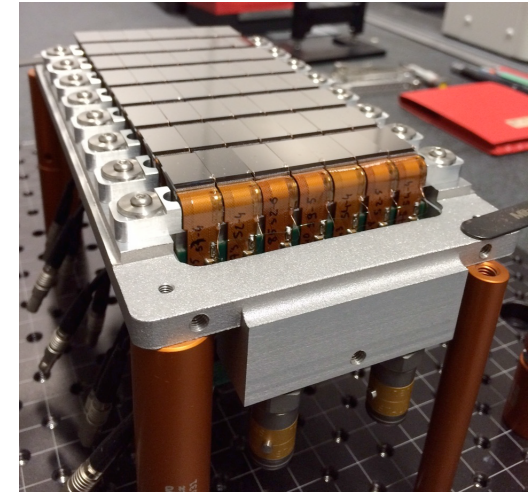
- **XPIX**: Development of the hybrid pixel detectors XPAD3.1 (2006) et XPAD3.2 (2009) with Si and CdTe sensors

- > 0,5 Mpixels $130 \times 130 \mu\text{m}^2$
- 240 images/s

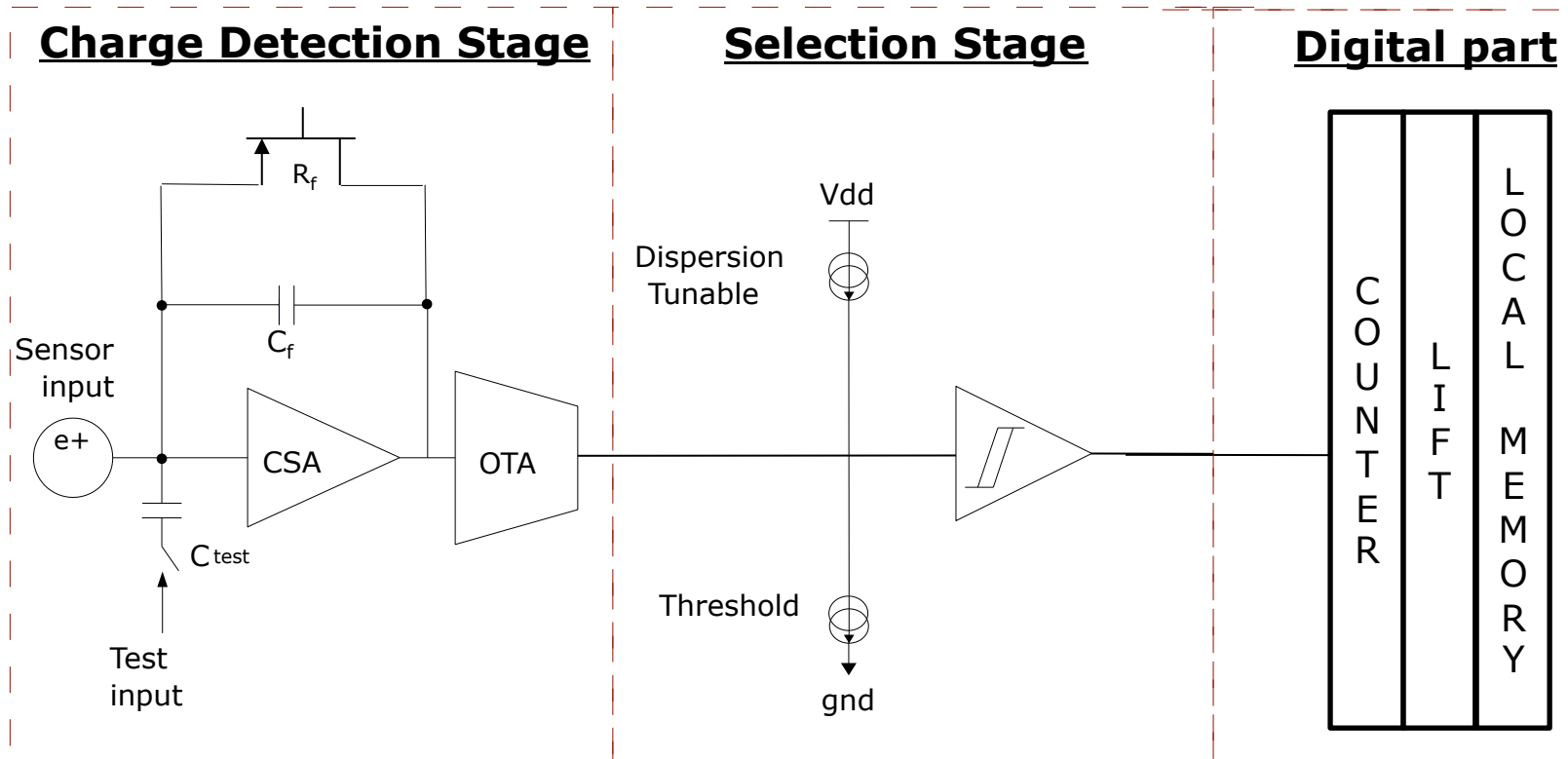
- 2011 • 5-35 keV (XPAD3.1/Si: D1-3)
- 2013 • 5-60 keV (XPAD3.2/Si: D4-6)

CHiPSpeCT

- 2015 • XPAD3.2/CdTe (D7)



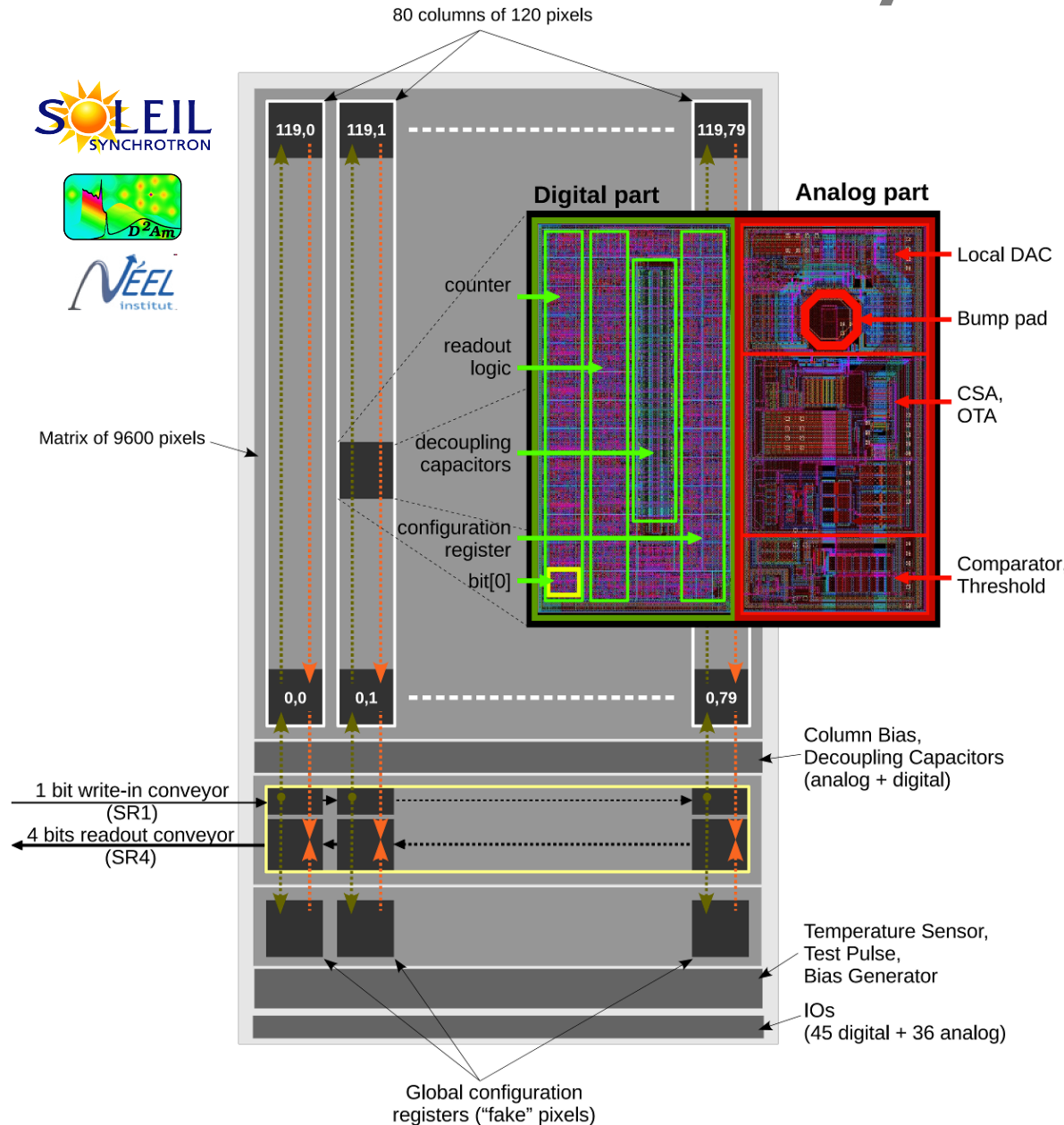
XPAD3 pixel architecture



Gain : 89 nA/keV
 Noise : 127 e⁻ rms
 Linearity : < 10% @ 35 keV

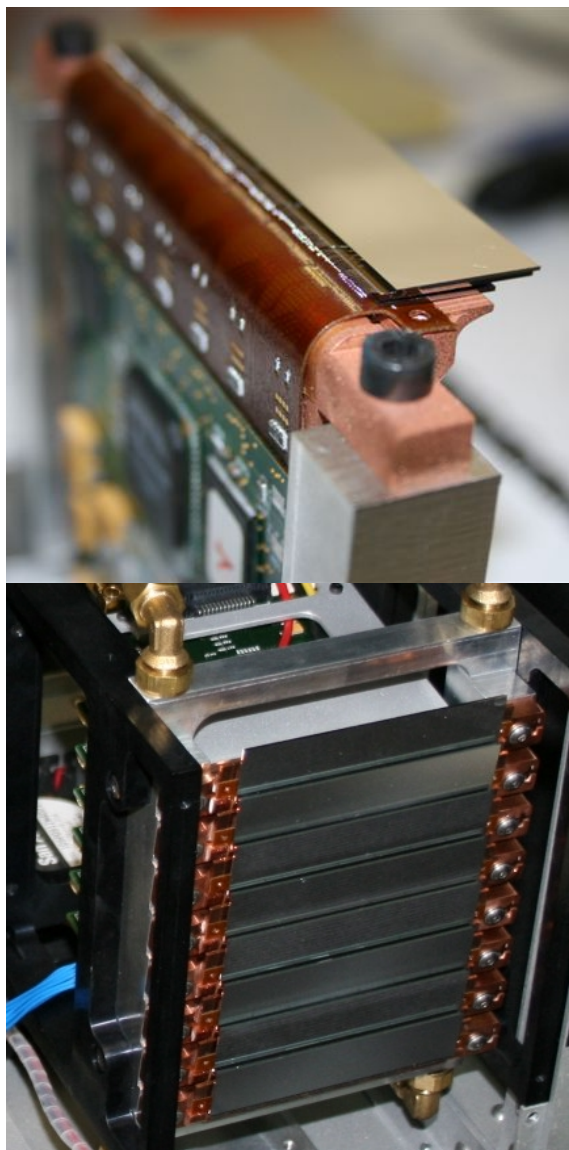
Power consumption : 40 μW/pixel
 Threshold adjustment resolution : 57 e⁻
 Minimum threshold: < 4 keV

XPAD3: Si and CdTe Hybrid Pixels for X-ray



- 0.25 μm IBM CMOS technology
- $(130 \times 130) \mu\text{m}^2$ pixels
- $80 \times 120 = 9600$ pixels
- 12 bit counter + overflow
- Count rate up to 10^6 ph/pixel/s
- < 1 ms readout time
- 5-35 keV adjustable thresholds

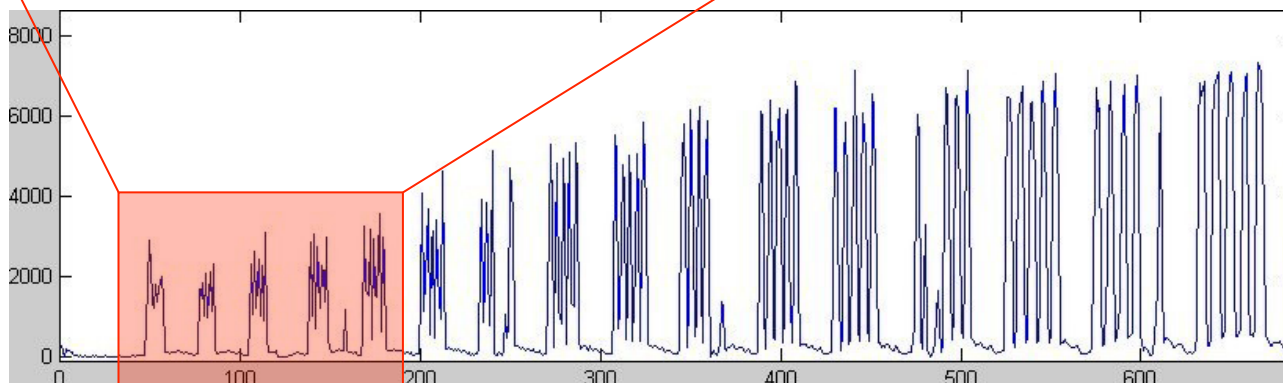
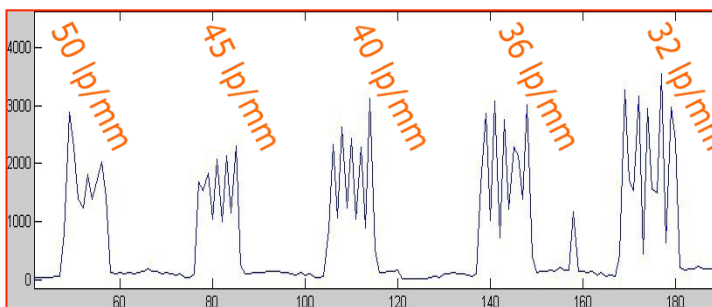
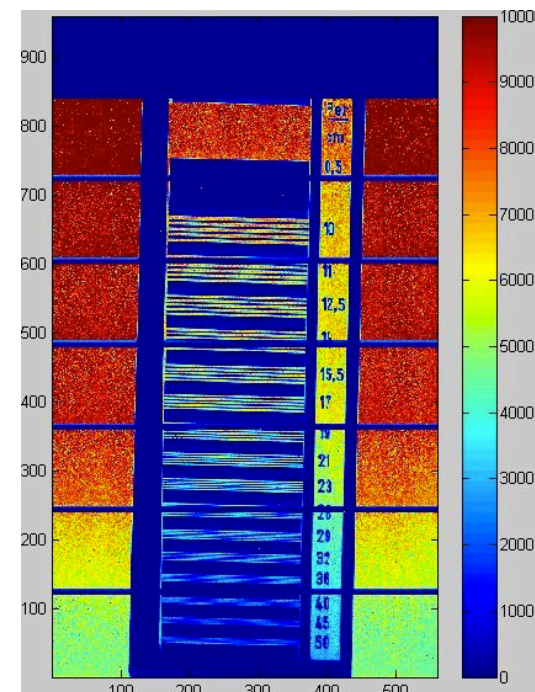
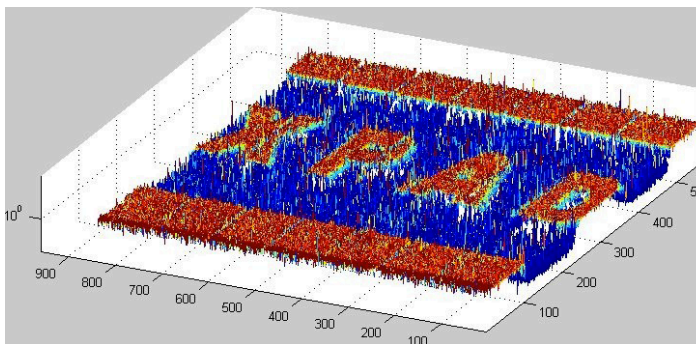
XPAD3 Camera : 500,000 pixels of 130 μm



5 keV



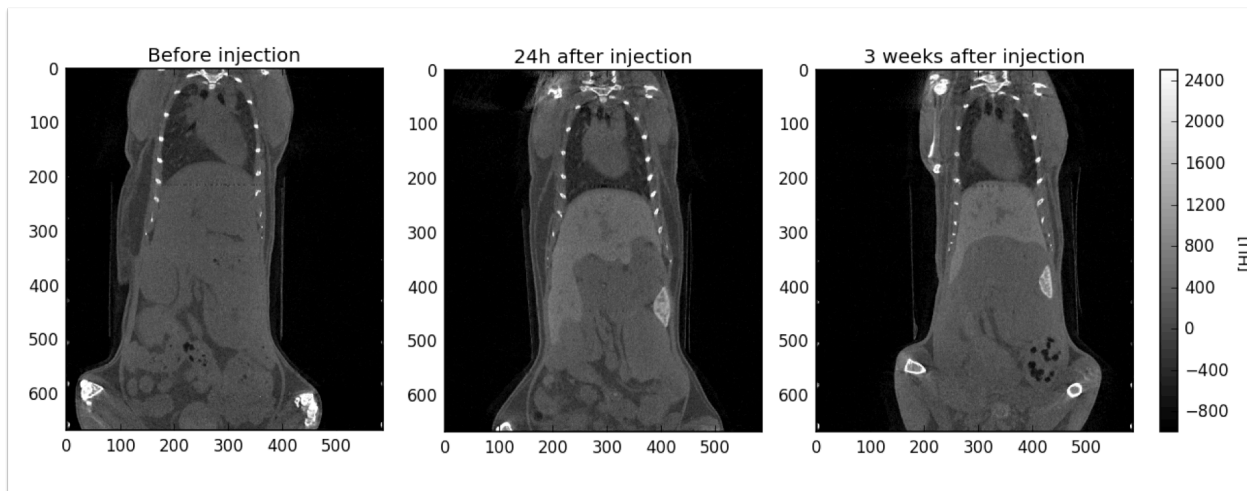
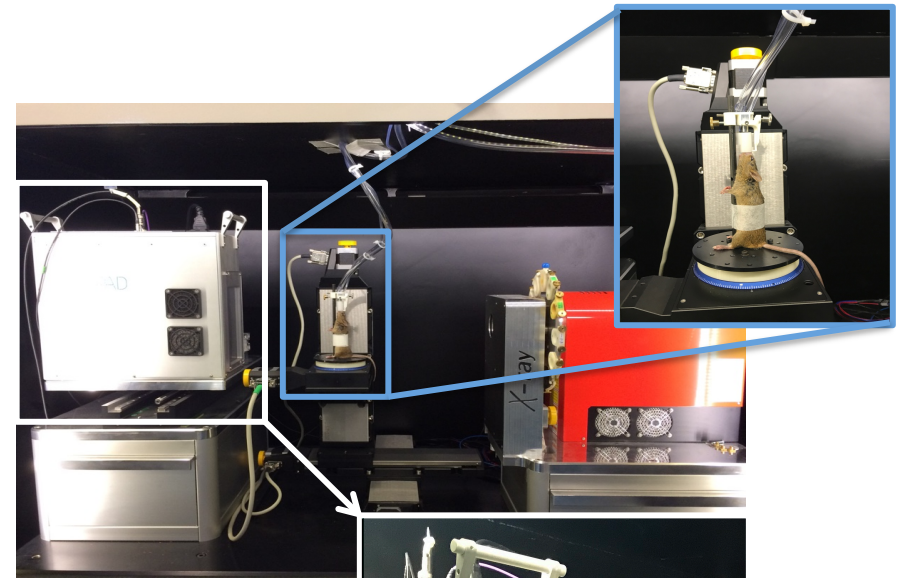
14 keV



First longitudinal study of liver tumour development in mice

In vivo imaging protocole

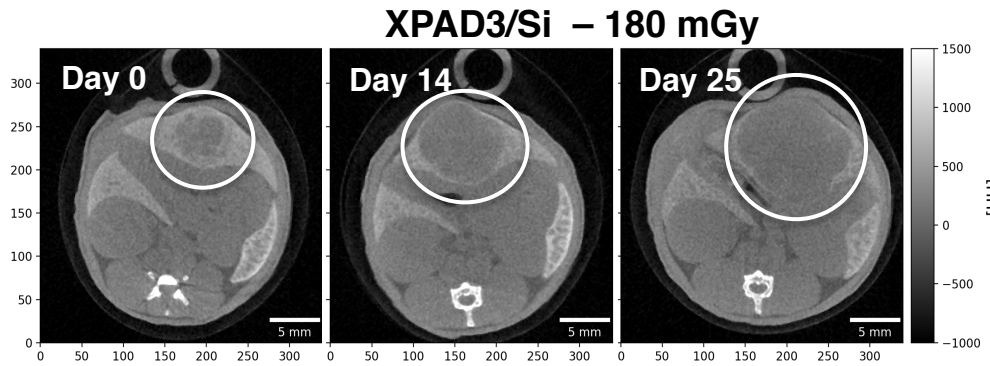
- Standard absorption imaging
- Anaesthesia: 3 % Isoflurane
- Source: 50 kV/500 μ A/0.6 mm Al
- Scan type: continuous
- Exposition duration: 575 ms + 50 ms DT
- Projections: 720 (0.5°)
- Delivered dose: 177 mGy/acquisition



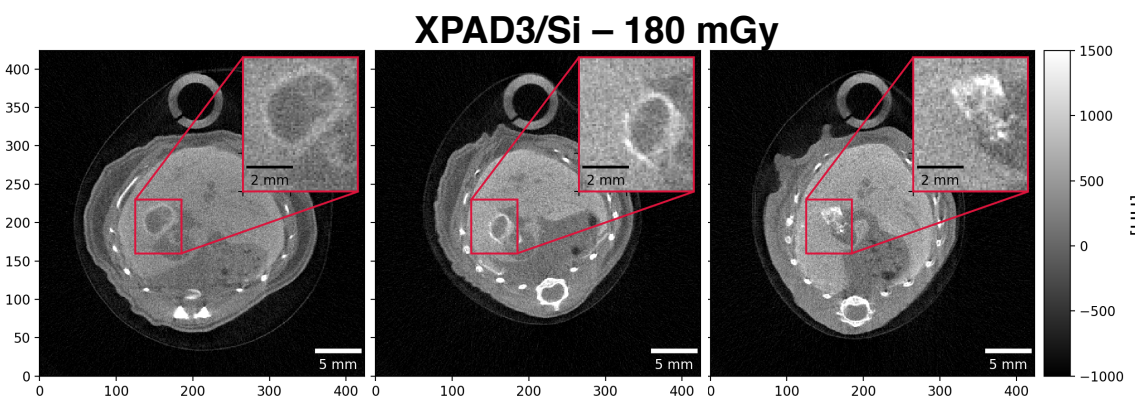
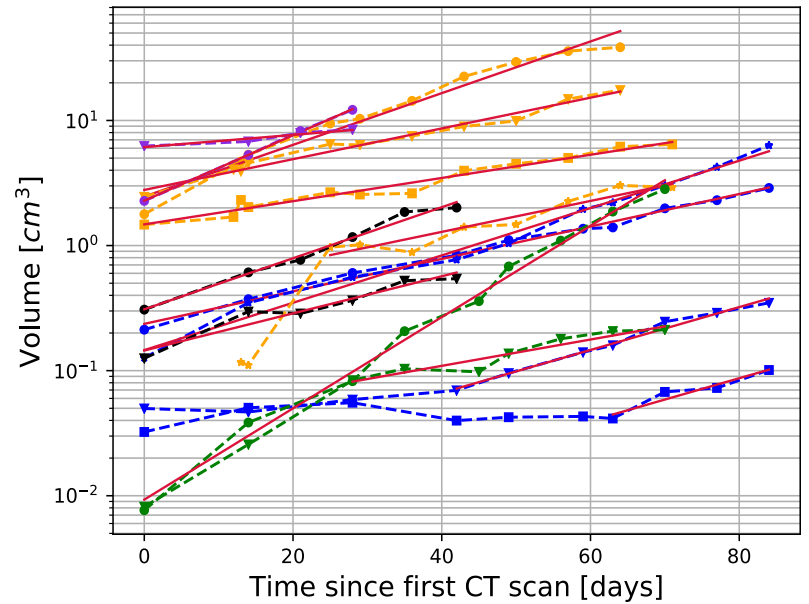
Coronal slices of a the same mouse labelled with 100 μ L/30g of Exitron nano 12000

Ecole d'été Franco-Chinoise, Marseille, 2-10 Jul 2018

First longitudinal study of liver tumour development in mice



Follow up of a mouse with an hepatocellular carcinoma for one month



Monitoring of the treatment response to an hepato-specific therapy (Mek + Bcl-XL inhibition*) for 40 days

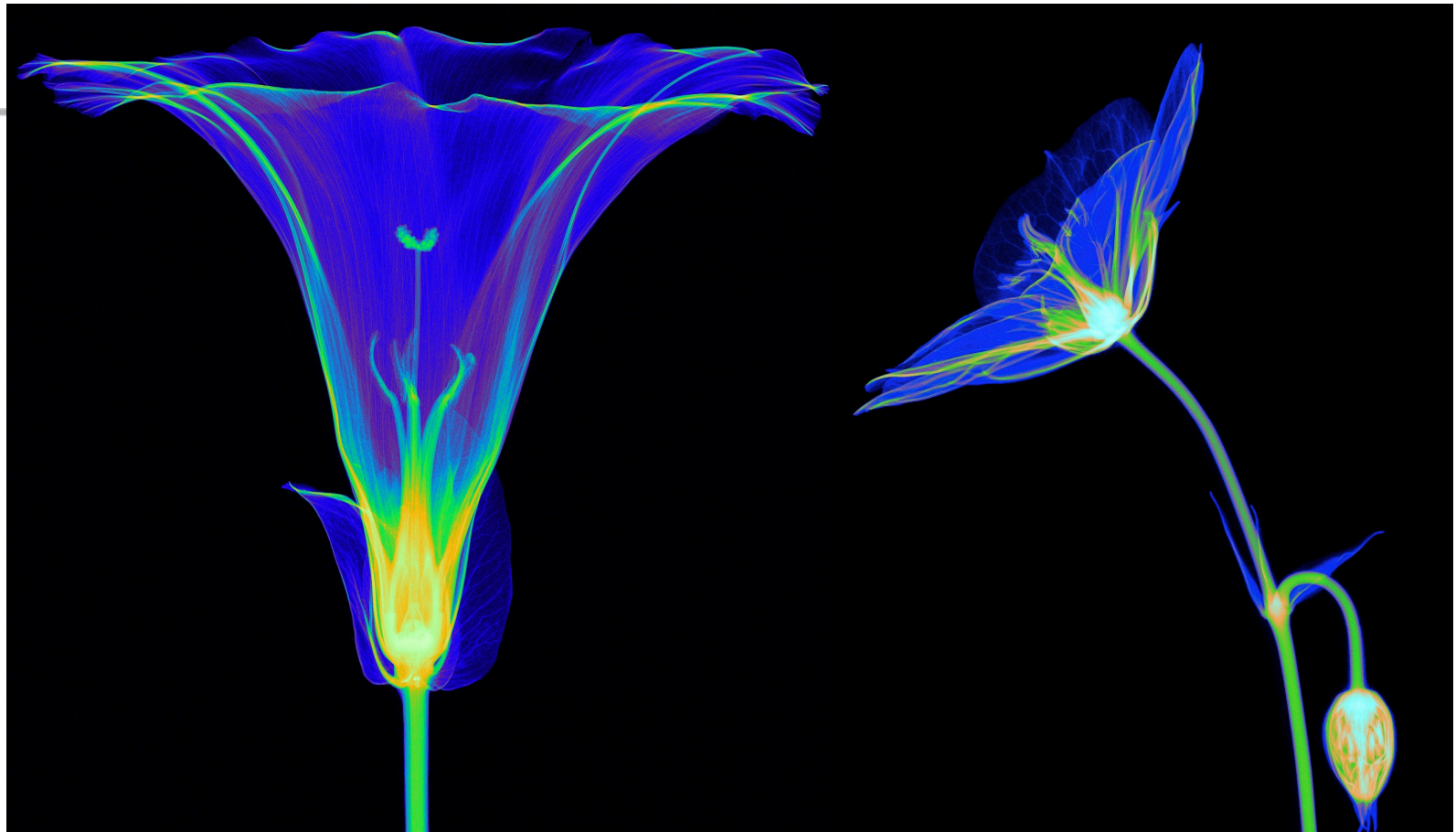
*Y. Fan et al., Hepatology 66 (2017)



Name	Matrix	side (μm)	Energy thresholds	Peaking time (ns)	Maximum count rates (Mcps/pixel)	Maximum count rates (Mcps/mm ²)	Electronics Noise or energy resolution	Power per channel (μW)	CMOS node
Medipix3 (FPM-SPM) ¹	256x256	55	2	120	2.5	826.5	1.37keV FWHM @ 10keV	7.5	0.13 μm
Medipix3 (FPM-CSM) ²	256x256	55	1+1	120	5.0E-01	163.5	2.03keV FWHM @10keV	9.3	0.13 μm
Timepix3 (CERN) ³	256x256	55	10bits	30	1.6E-03	0.53	4.07keV FWHM at 59.5keV	15.2	0.13 μm
Pixirad Pixie II ⁴	512x476	55.6	2	300	5.0E-01	161.5	1.45keV FWHM @ 20keV	12.5	0.18 μm
Samsung PC ⁵	128x128	60	3	NS	NS	NS	68 e- r.m.s.	4.6	0.13 μm
Pixirad Pixie III ⁶	512x402	62	2	125	1.0	260.1	6.6% FWHM @ 60keV	34	0.16 μm
Eiger ⁷	256x256	75	1	30	4.2	711.1	121e- r.m.s. (low noise settings)	8.8	0.25 μm
PXD23K (AGH) ⁸	128x184	75	2	48	8.5	1519.5	89e- r.m.s.	25	0.13 μm
X-Counter PC (PDT25-DE) ⁹	256x256	100	2	NS	1.2	120	8.3keV FWHM @20keV 10keV FWHM @60keV	NS	NS
PXD18K (AGH) ⁸	96x192	100	2	30	5.8	580	168e- r.m.s.	23	0.18 μm
FPDR90 (AGH) ⁸	40x32	100	2	28	8.5	854.7	106e- r.m.s.	42	90nm
AGH_Fermilab ¹⁰	18x24	100	2	48	NS	NS	84e- (Single pixel), 168e- (Charge summing)	34	40nm
Medipix3 (SM-SPM) ¹¹	128x128	110	8	120	4.5	375.7	1.43keV FWHM @ 10keV	30	0.13 μm
Medipix3 (SM-CSM) ¹²	128x128	110	4+4	120	3.4E-01	28.1	2.2keV FWHM @10keV	37.2	0.13 μm
XPAD3 ¹³	80x120	130	2	150	2.0	118.3	127e- r.m.s.	40	0.25 μm
Pilatus 2 ¹⁴	60x97	172	1	110	6.0	202.8	1keV FWHM @ 8keV	20.2	0.25 μm
Pilatus 3 ¹⁵	60x97	172	1	110	15.0	507.0	1keV FWHM @ 8keV	20.2	0.25 μm
Telesystems ¹⁶	40x40	200	4	300-500	8.0E-01	20	5.36keV FWHM @ 122keV	94.4	0.25 μm
Dosepix (CERN) ¹⁷	16x16	220	16	287	1.6	33.9	150 e- r.m.s.	14.6	0.13 μm
Siemens PC ¹⁸	64x64	225	2	20	40.0	790.1	NS	NS	NS
Hexitec ¹⁹	80x80	250	14bits	2000	1.0E-03	0.016	800eV FWHM @ 60keV, 1.1keV @ 141keV	220	0.35 μm
Philips Chromaix ²⁰	4x16	300	4	20	38.0	422.2	4.7keV @60keV (1 channel)	3000	0.18 μm
Ajat-0.35 (PC) ²¹	32x64	350	1	1000	2.2	18.0	4keV FWHM @122keV	390.6	0.35 μm
Ajat-0.35 (ADC) ²²	32x64	350	64	1000	4.9E-05	4.0E-04	4keV FWHM @122keV	390.6	0.35 μm
CIX 0.2 (Bonn) ²³	8x8	353.6	1	NS	12.0	96	330e- r.m.s. (counting channel)	3200	0.35 μm
KTH_Lin_SPD ²⁴	160 ch.	447.2	8	10-20-40	272.0	1360	1.09keV @ 15keV (measured at 40kcps)	80000	0.18 μm
DxRay-Interon ²⁵	16x16	500	4	10	13.3	53	7keV FWHM @60keV, Min TH20keV	NS	NS
Ajat-0.5 ²⁶	44x22	500	2	1000-2000	NS	NS	4.7keV @122keV (1 channel)	413.2	0.35 μm
Hamamatsu ²⁷	64 ch.	632.5	5	NS	5.5	13.75	12keV FWHM @ 120keV	NS	NS
IDEAS ²⁸	64 ch.	894.4	6	50	4.0	5	7keV FWHM @60keV	4200	0.35 μm
GE-DxRay ²⁹	128 ch.	1000	2	30	11.6	11.6	4.75% at 122keV, CZT, 5pF Cin (1 Channel noise= 4.8keV FWHM)	2100	0.25 μm
BNL ³⁰	64 ch.	1241.0	5	40-80-160-320	4.0	5.5	5.5keV at 40ns peaking time/2.15keV at 320ns peaking time	4700	0.25 μm

Courtesy: R. Ballabriga, Medipix Collaboration, CERN

Medipix3/Si RX images



Courtesy: S. Procz, Medipix Collaboration, CERN

- Medipix3/Si 55 μ m SPM HGM 24-Bit, 8 x 8 tiles
- 20kV / 100 μ A, Mag. 2x
- Object width \sim 45 mm

Ecole d'été Franco-Chinoise, Marseille, 2-10 Jul 2018



Hybrid pixels: many spin-offs

2003



www.dxray.com

2006



www.dectris.com

2010



www.imxpad.com

2011



pixirad.pi.infn.it

2006

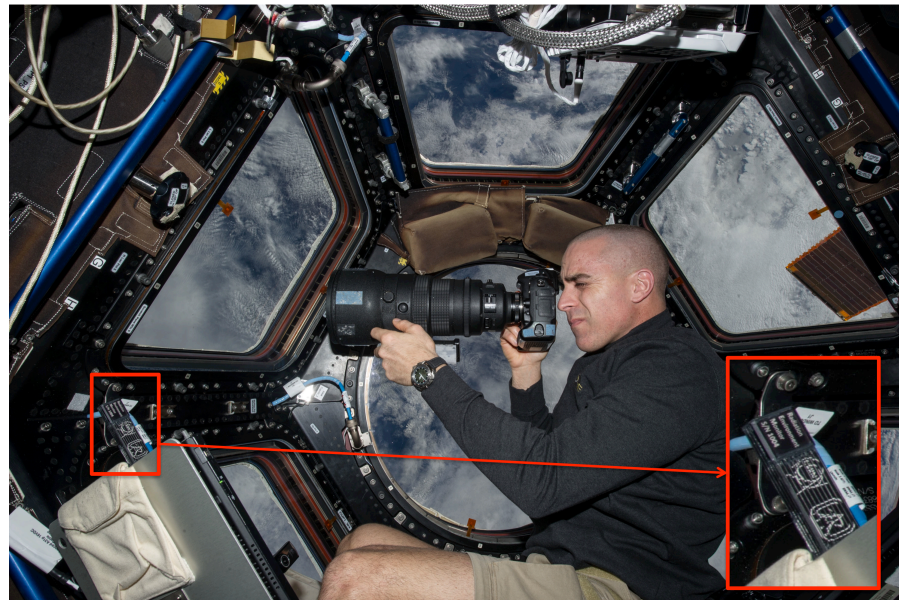


Pixelated X-Ray Detectors
www.xray-imatek.com

2011



www.amscins.com



Courtesy: NASA, photo ref. no. iss036e006175

2003

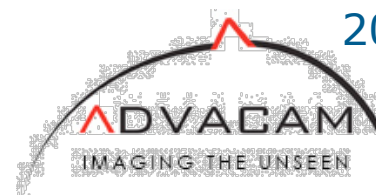


www.kromek.com

2007



www.marsbioimaging.com



www.advacam.com

2012

2011

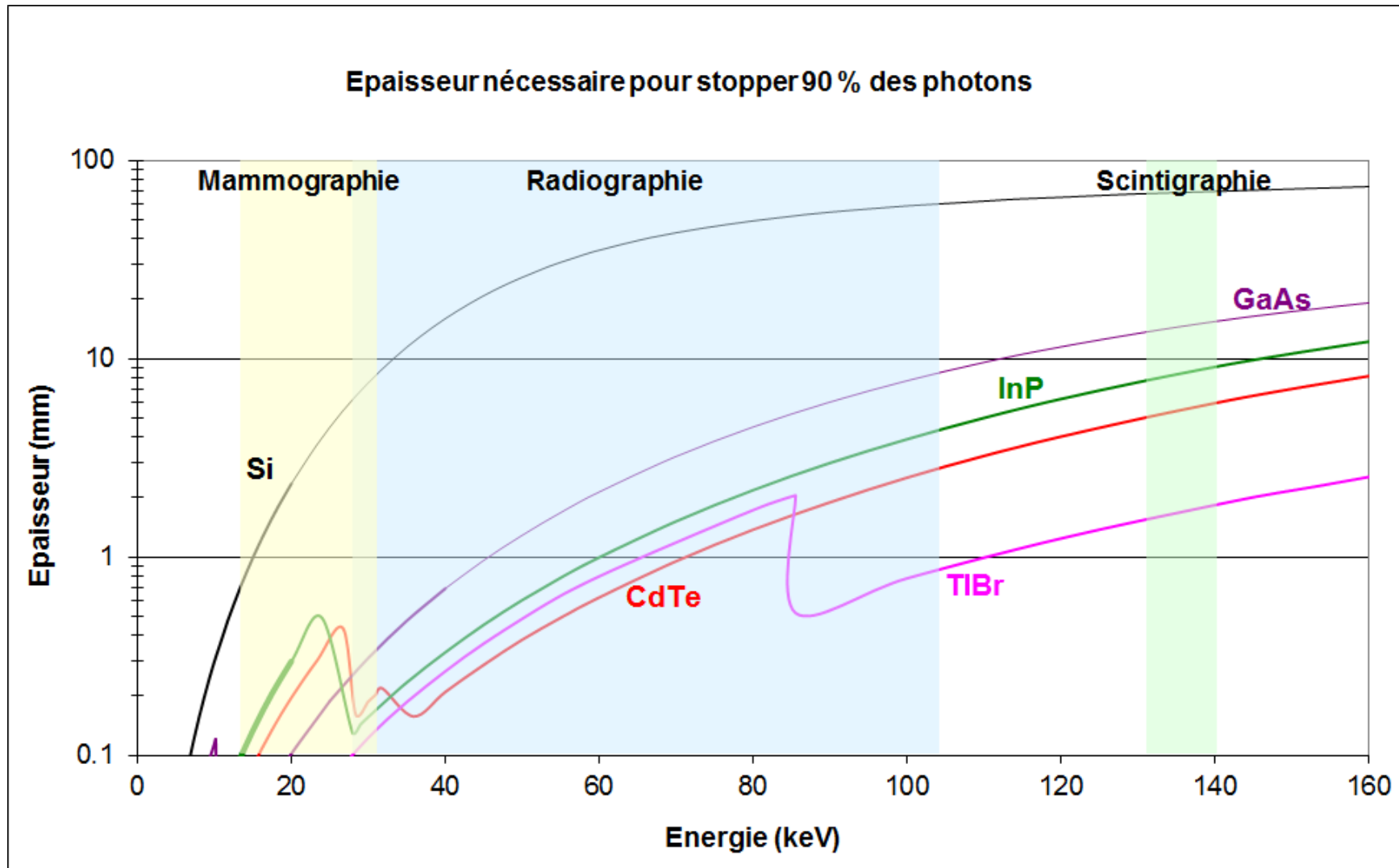


www.xi-europe.com

Ecole d'été Franco-Chinoise, Marseille, 2-10 Jul 2018



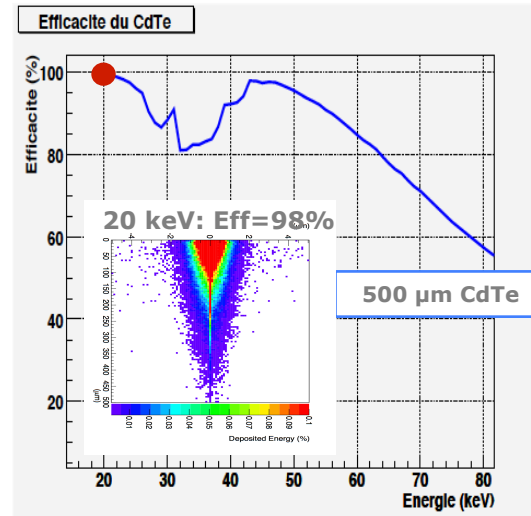
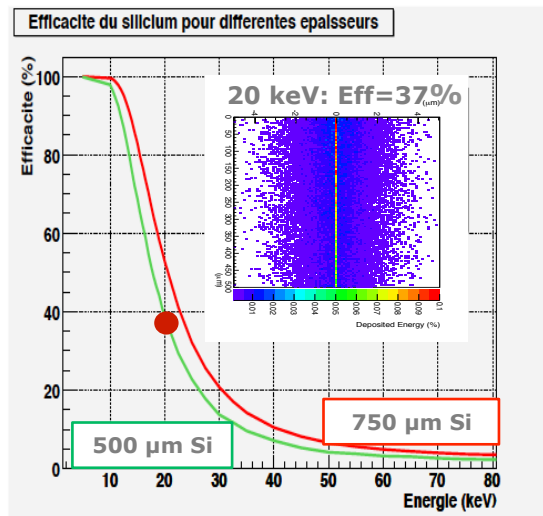
Sensors for direct X-ray detection



Courtesy: E. Gros d'Aillon, CEA-LETI

Quelles sont les differences ?

	Z	P (g/cm ³)	E ₀ (eV)	E _p (eV)	μ _e (cm ² /V/s)	τ _e (s)	μ _h (cm ² /V/s)	T _h (s)	μ _e T _e (cm ² /V)	μ _h T _h (cm ² /V)
Diamond	6	3.52	5.5	13.0	4500		3800			
Si	14	2.32	1.12	3.62	1400	1×10 ⁻³	480	2×10 ⁻³	1.4	0.96
Ge	32	5.33	0.67	2.95	3900	1×10 ⁻³	1900	1×10 ⁻³	3.9	1.9
GaAs	32	5.32	1.43	4.30	8000	1×10 ⁻⁸	400	1×10 ⁻⁷	8×10 ⁻⁵	4×10 ⁻⁵
Cd _{0.9} Zn _{0.1} Te	49.1	5.78	1.57	4.64	1000	3×10 ⁻⁶	50	1×10 ⁻⁶	3×10 ⁻³	5×10 ⁻⁵
CdTe	50	5.85	1.44	4.43	1100	3×10 ⁻⁶	100	2×10 ⁻⁶	3.3×10 ⁻³	2×10 ⁻⁴



K-edge Cd : 26.7 keV

K-edge Te : 31.8 keV

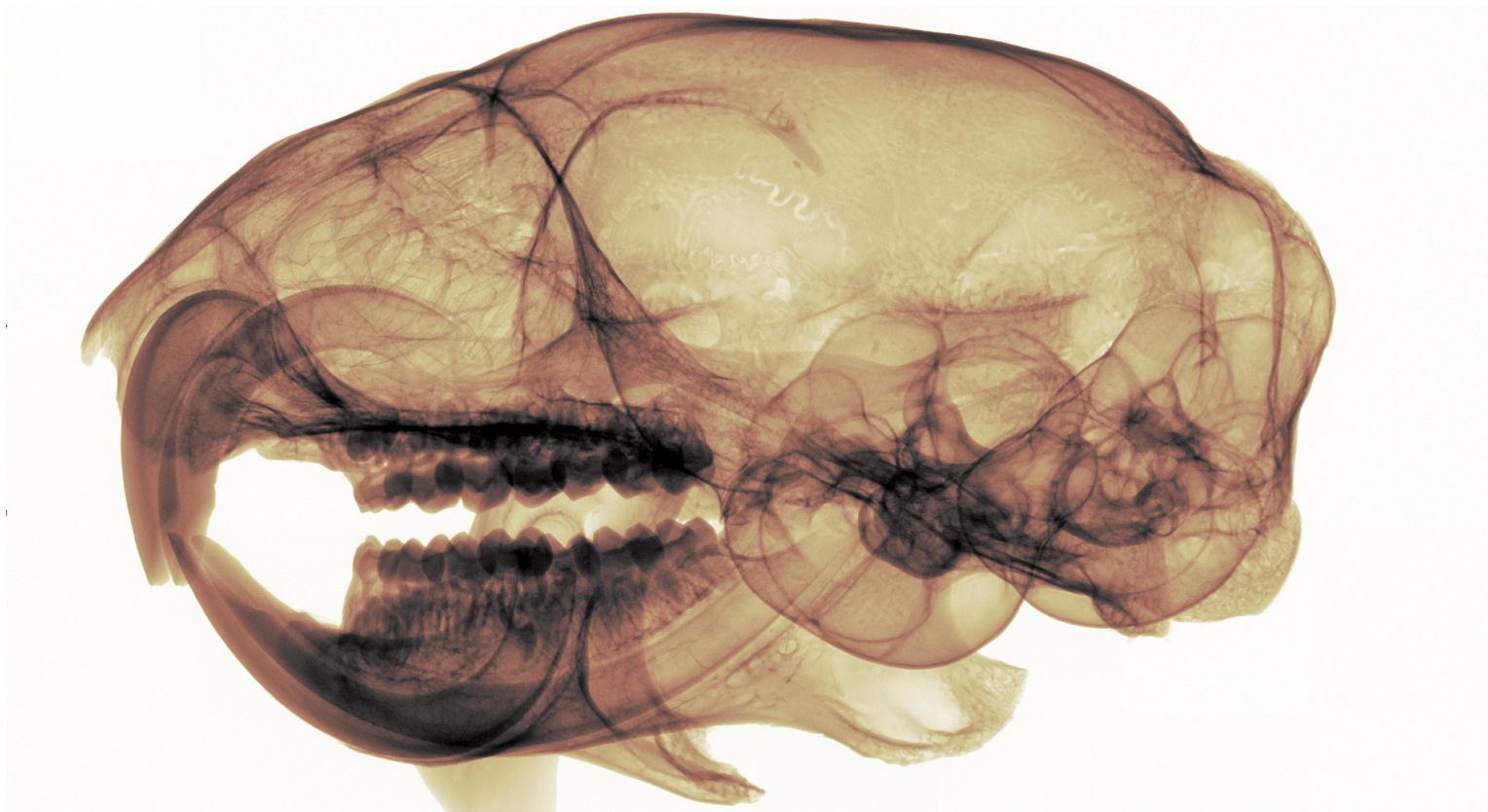
K-alpha Cd : 23.1 keV

K-alpha Te : 28.4 keV

Medipix3 Image (GaAs 55 $\mu\text{m}/500 \mu\text{m}$)

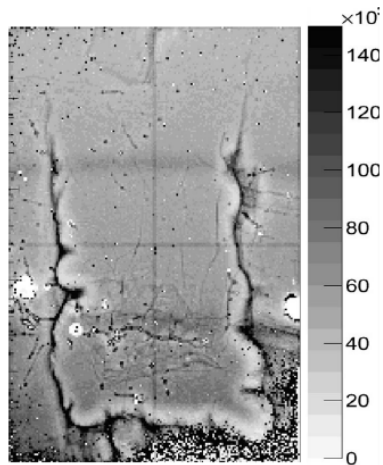


A tiled X-ray image of a mouse skull

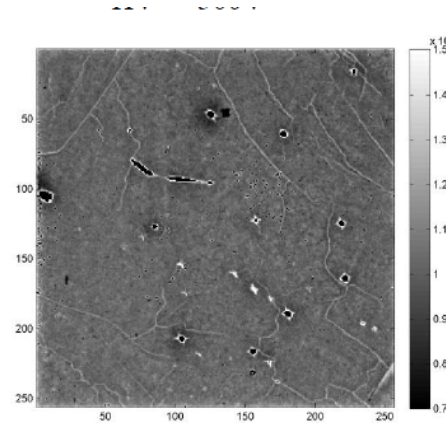


Courtesy: S. Procz, Medipix Collaboration, CERN

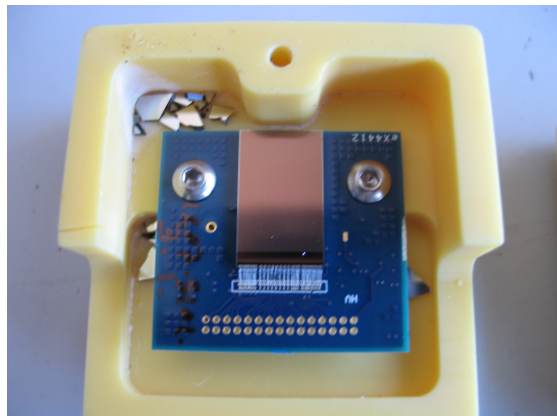
ChiPSpeCT & CALIPSO: XPAD3-2/CdTe camera



XPAD3 « Quad »



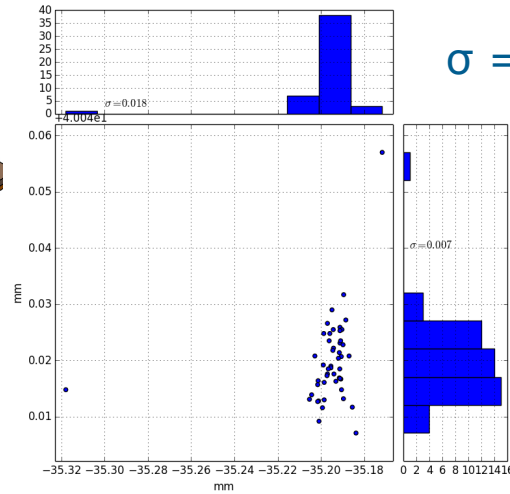
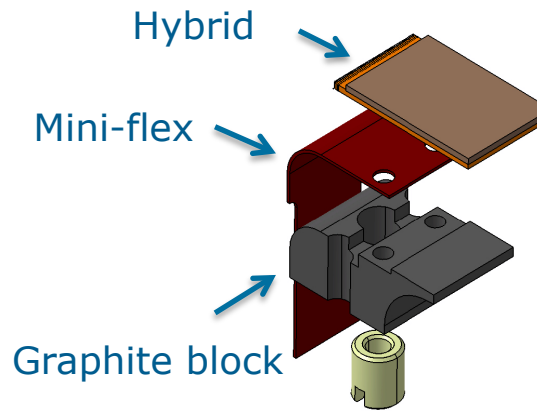
Medipix2 « Quad »



June 7 2013

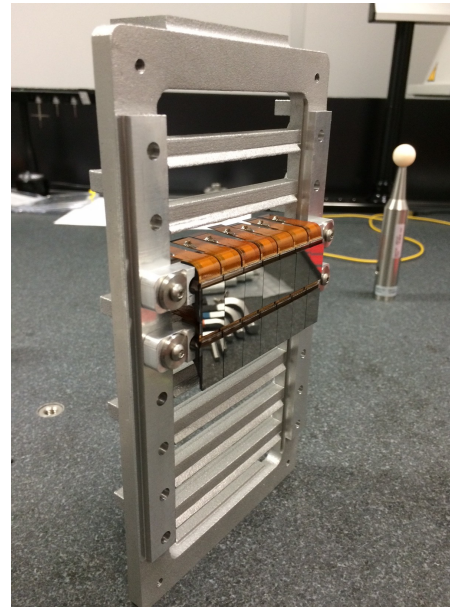
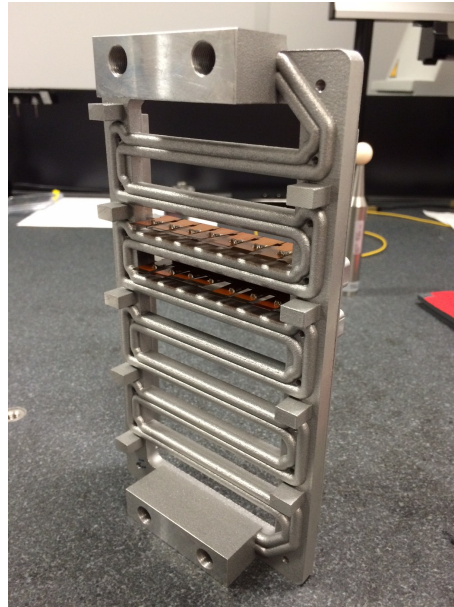
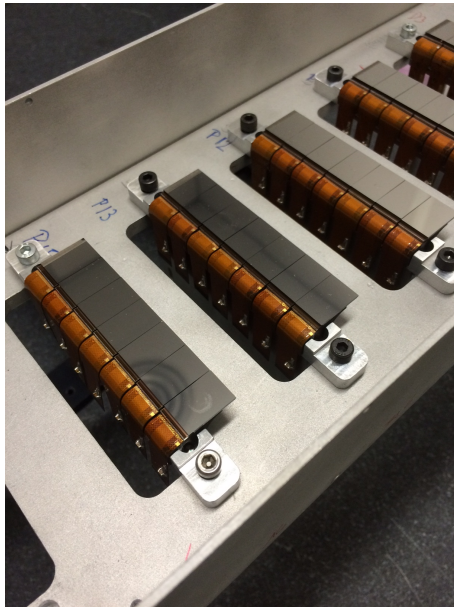
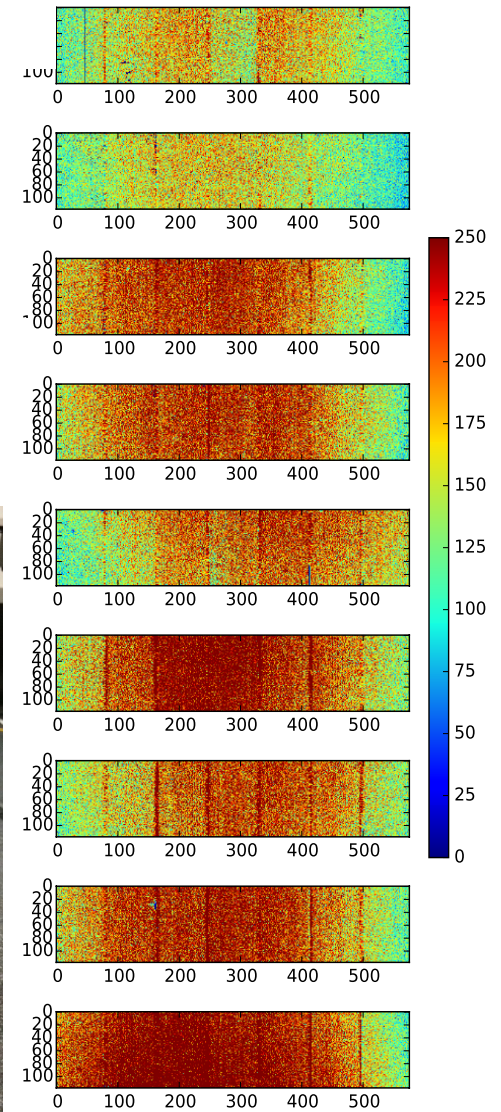
- ▶ HighZpad (FP7 ELISA)
 - ▶ « Survey » of state-of-the-art high-Z sensors and of hybridization methods to get large surface detectors
 - ▶ 3 pixel circuits considered (Medipix2, Pilatus, XPAD3)
 - ▶ One « hybridizer » : XIE, indium bumps
 - ▶ CdTe sensors for « Quads » (Acrorad)
 - ▶ For all the considered circuits, there were hybridization problems or impairing of sensors generating spots and high leakage currents.

Construction of the CHiPSpeCT camera

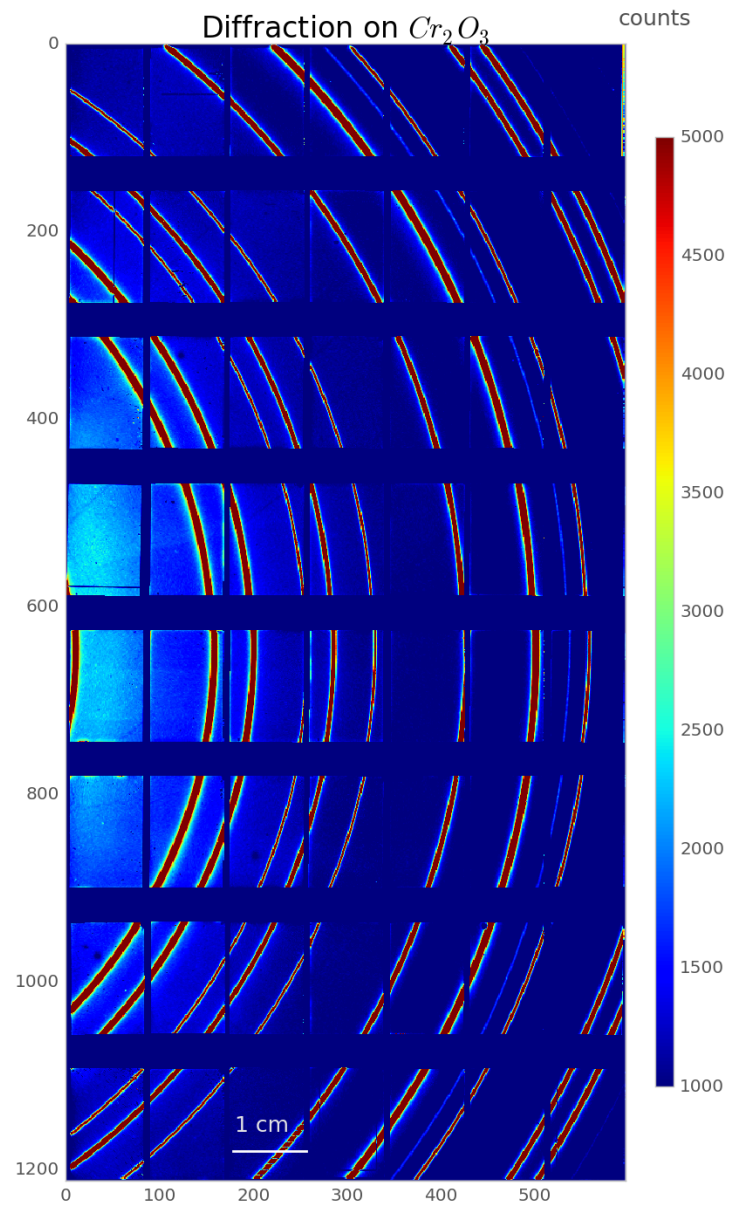
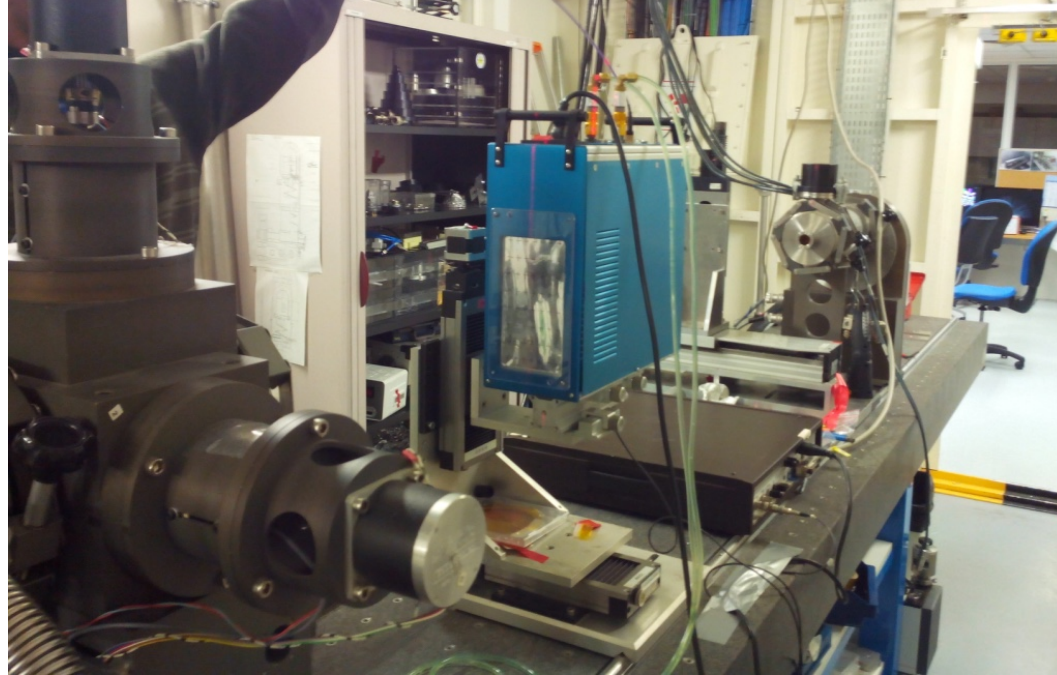
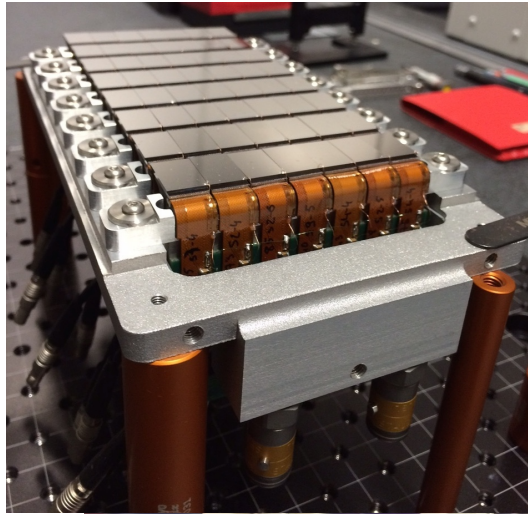


$\sigma = 0.018 \text{ mm}$

$\sigma = 0.007 \text{ mm}$



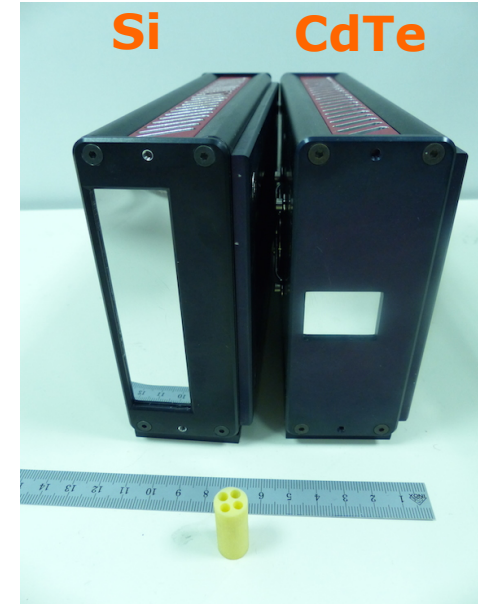
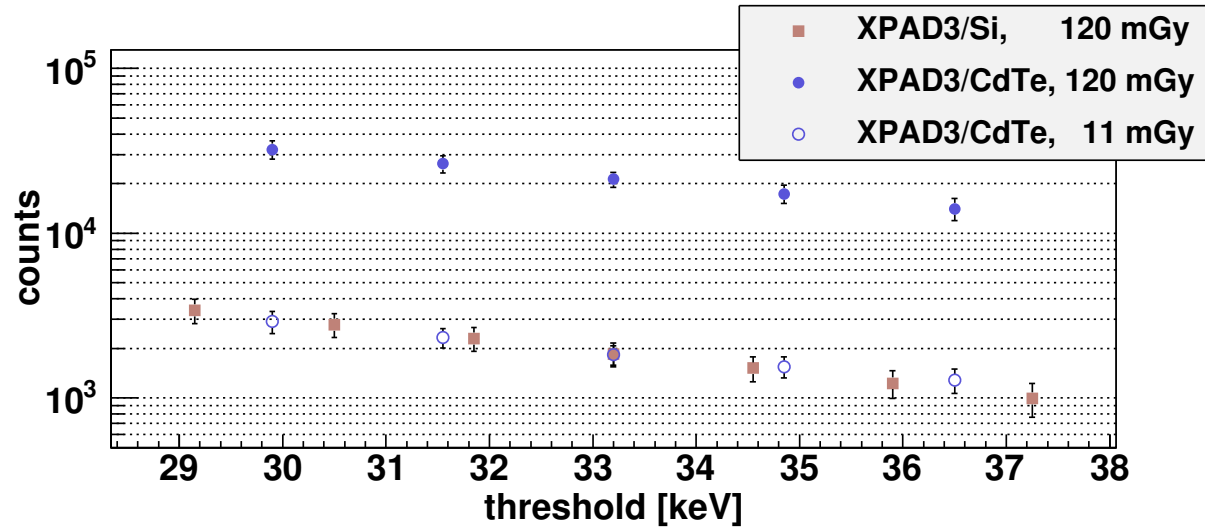
First irradiations on the D2AM ESRF beam line at at 25.5 keV



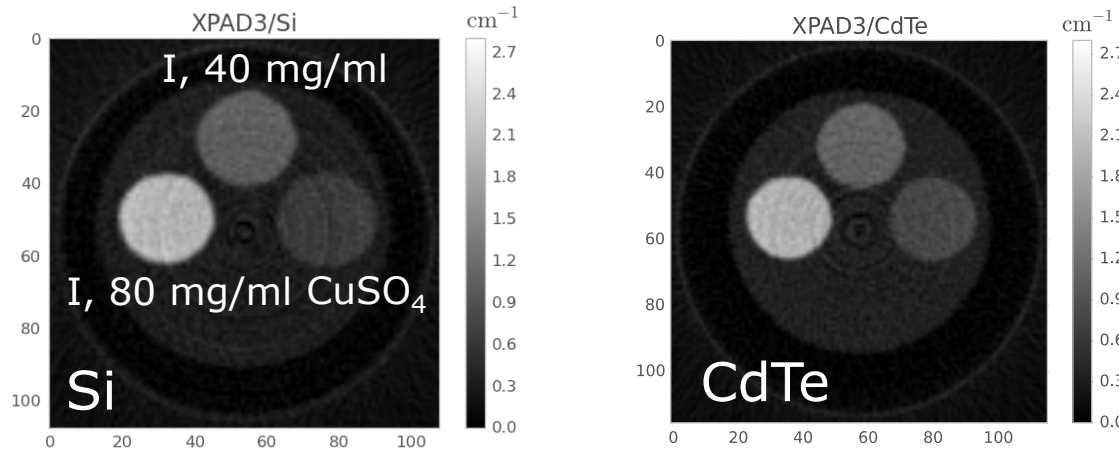
Ecole d'été Franco-Chinoise, Marseille, 2-10 Jul 2018

CdTe versus Si for standard absorption CT

➤ Dose reduction x 10 for $E > 30$ keV



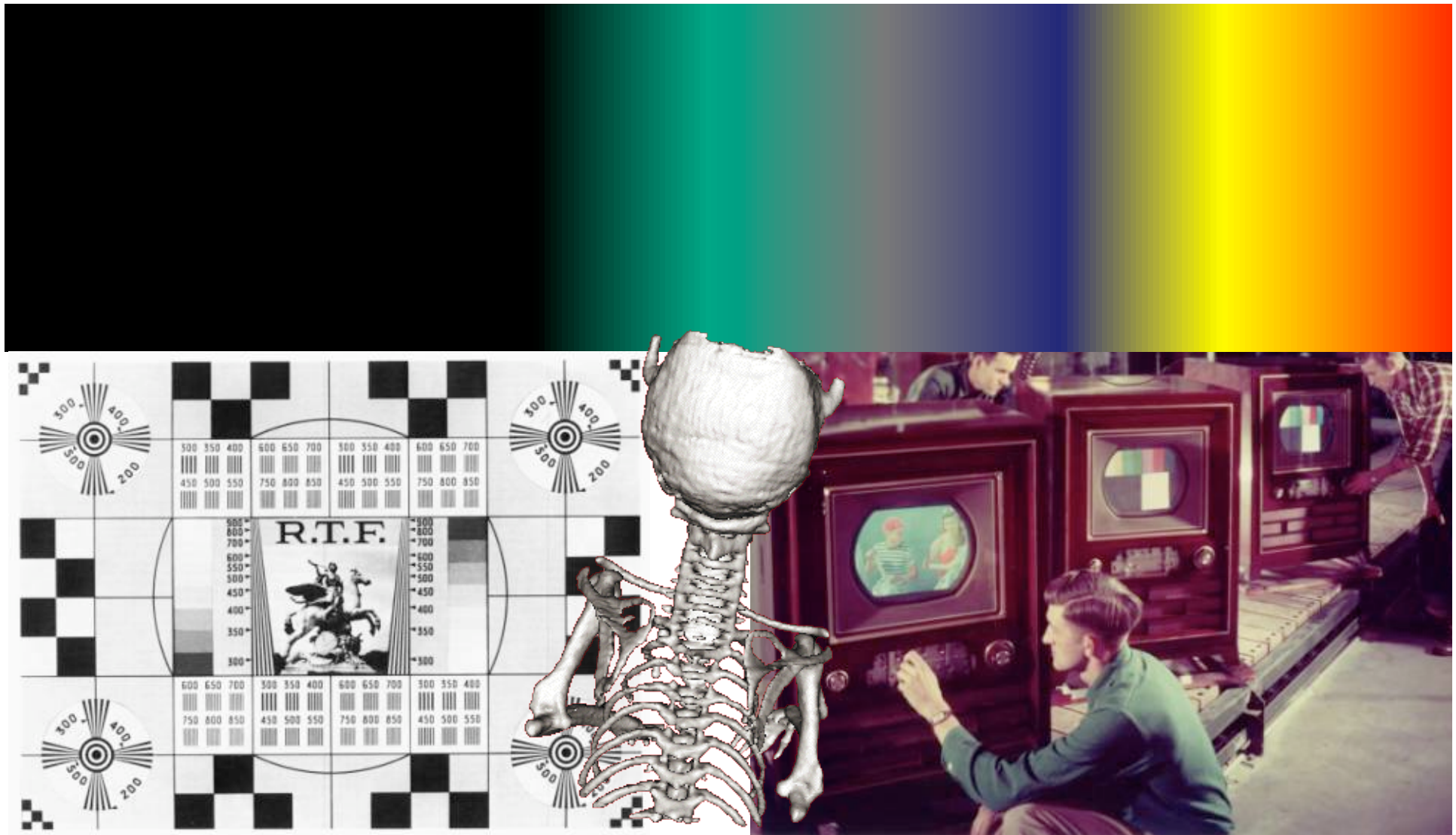
120 mGy → 11 mGy



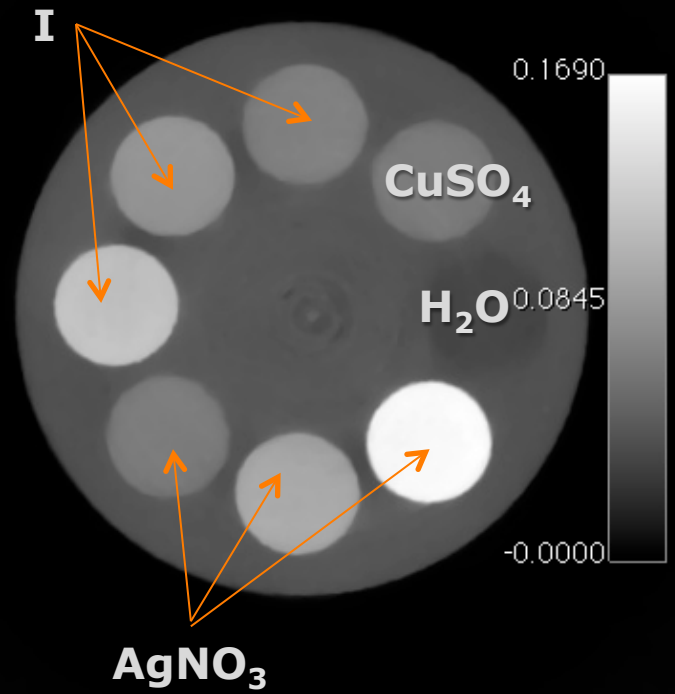
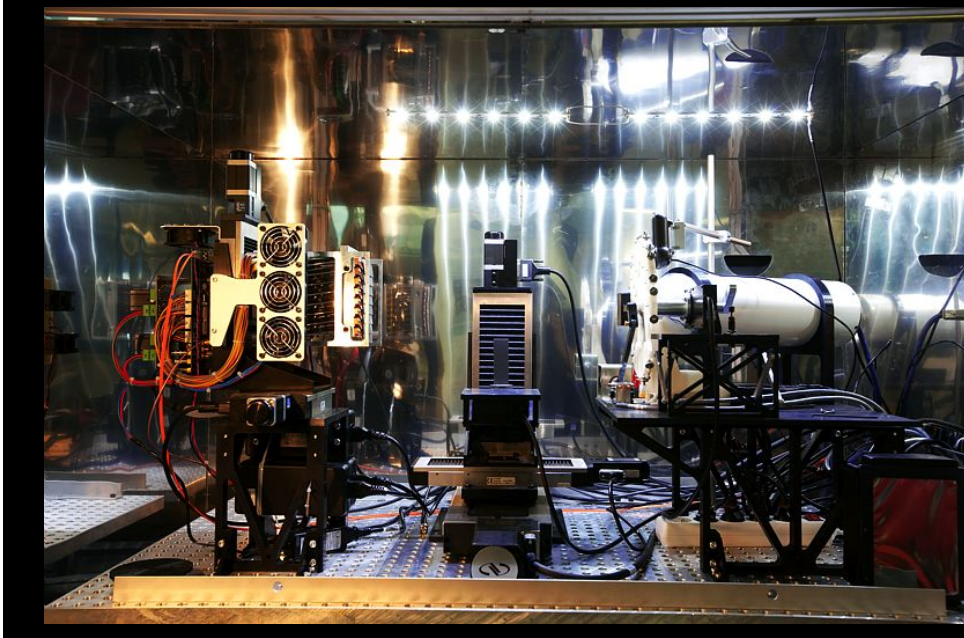
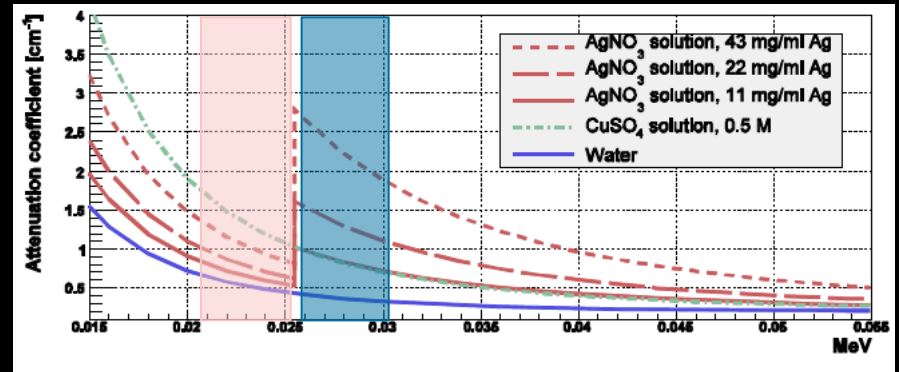
For equivalent stats

F. Cassol et al. Phys. Med. Biol. 60 (2015)

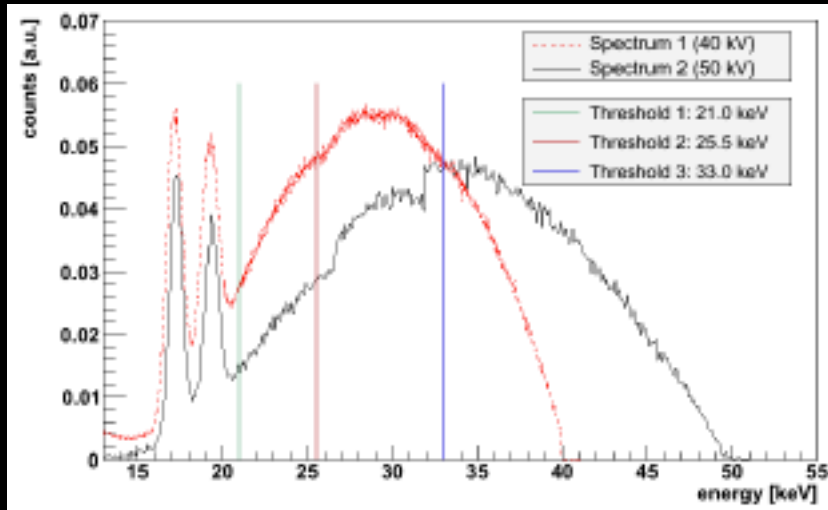
Spectral CT: from black & white to colour



Ecole d'été Franco-Chinoise, Marseille, 2-10 Jul 2018

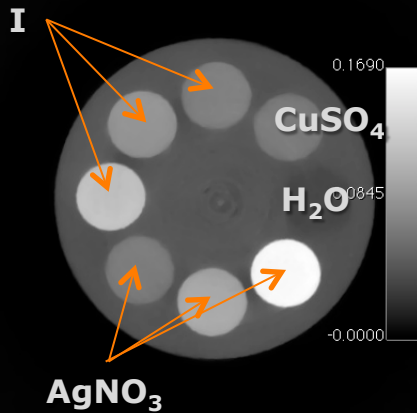


X-ray spectral CT using XPAD3

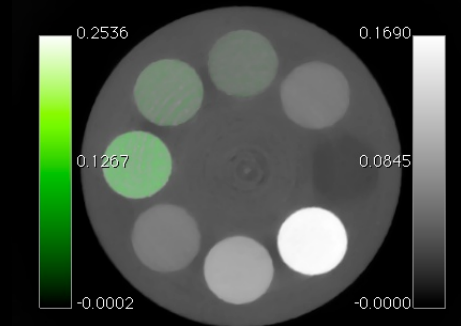


Silver	Iodine
$E_{1Ag} = 21 \text{ keV}$	$E_{1I} = 25.5 \text{ keV}$
$E_{2Ag} = 25.5 \text{ keV}$	$E_{2I} = 33 \text{ keV}$
$E_{3Ag} = 33 \text{ keV}$	$E_{3I} = 40/50 \text{ keV}$

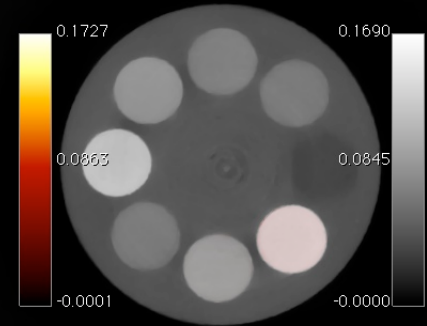
Standard CT



Iodine and Silver K-edge imaging



$$(E_{2I} - E_{3I}) - (E_{1I} - E_{2I})$$



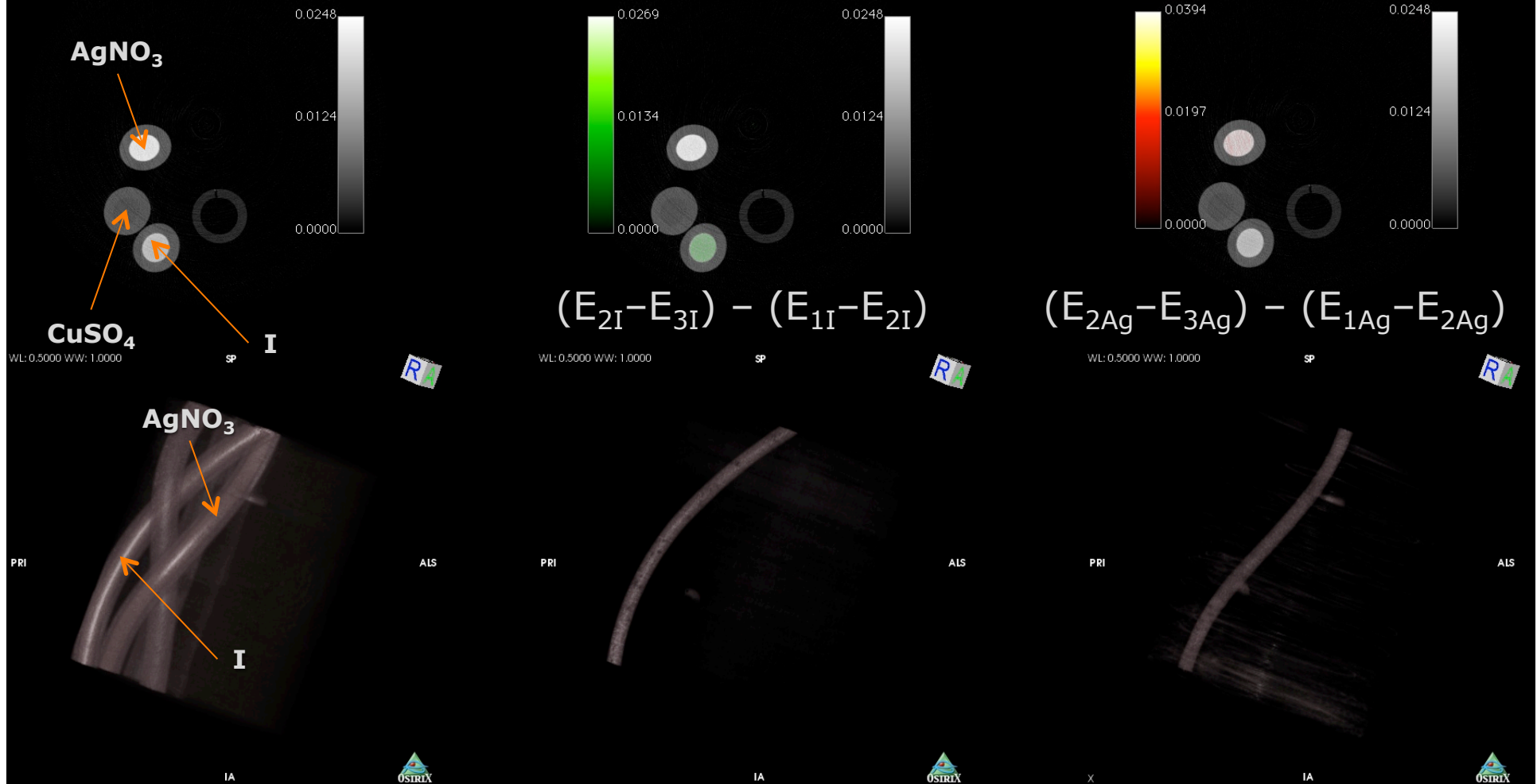
$$(E_{2Ag} - E_{3Ag}) - (E_{1Ag} - E_{2Ag})$$

Cassol *et al.*, IEEE Trans. Nucl. Sci. 60 (2013) 103

X-ray spectral CT using XPAD3

Standard CT

Iodine and Silver K-edge imaging

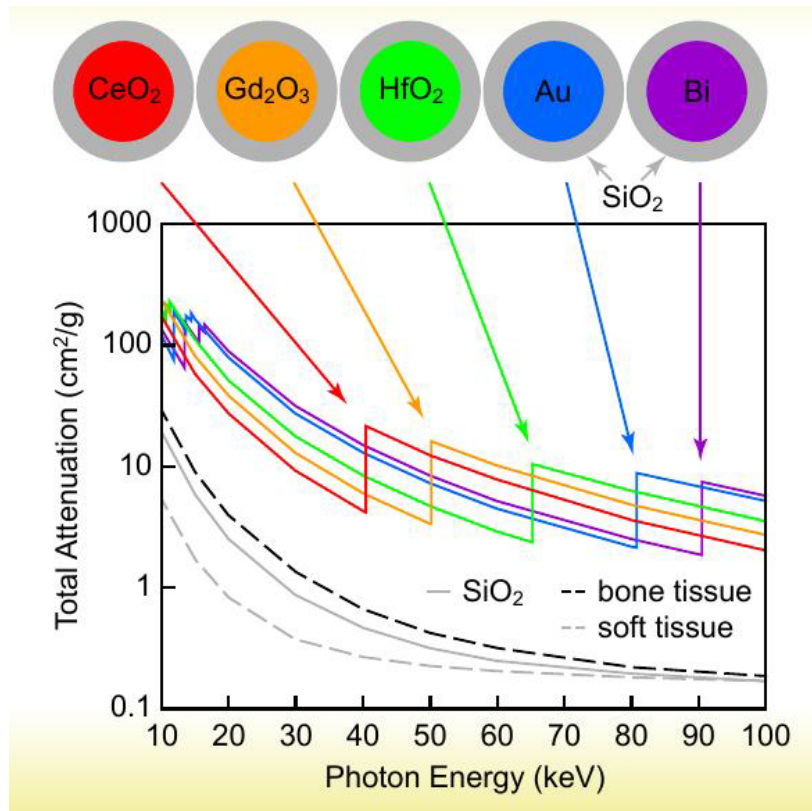


Cassol *et al.*, IEEE Trans. Nucl. Sci. 60 (2013) 103

Ecole d'été Franco-Chinoise, Marseille, 2-10 Jul 2018

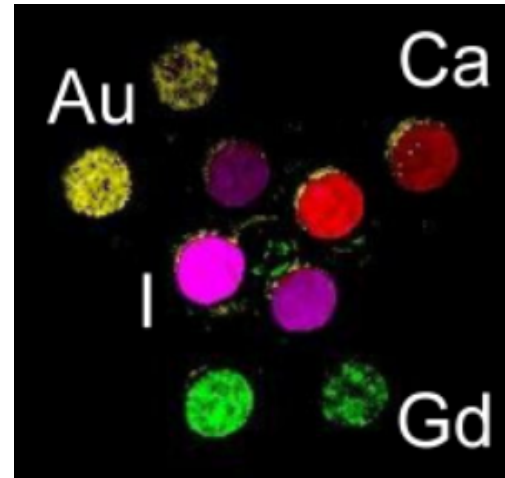


Spectral CT: a novel intrinsically anatomico-functional modality



L.E. Cole et al. Nanomedicine 10 (2015) 321

K-edge imaging of iodine using composite pixels with XPAD3



MARS image using human energy range (CdTe-MedipixRX)

Courtesy: A Buttler, Medipix Collaboration, CERN

